

35. VOLCANIC ASH FROM CELEBES AND SULU SEA BASINS OFF THE PHILIPPINES (LEG 124): PETROGRAPHY AND GEOCHEMISTRY¹

André Pouclet,² Manuel Pubellier,³ and Piera Spadea⁴

ABSTRACT

During Leg 124, off the Philippines, volcanic material was recovered in deep-sea sediments dating from the late Oligocene in the Celebes Sea Basin, and from the early Miocene in the Sulu Sea Basin. Chemical and petrological studies of fallout ash deposits are used to characterize volcanic pulses and to determine their possible origin. All of the glass and mineral compositions belong to medium-K and high-K calc-alkaline arc-related magmatic suites including high-Al basalts, pyroxene-hornblende andesites, dacites, and rhyolites.

Late Oligocene and early Miocene products may have originated from the Sunda arc or from the Sabah-Zamboanga old Sulu arc. Late early Miocene Sulu Sea tuffs originated from the Cagayan arc, whereas early late Miocene fallout ashes are attributed to the Sulu arc. A complex magmatic production is distinguished in the Plio-Quaternary with three sequences of basic to acidic lava suites. Early Pliocene strata registered an important activity in both Celebes Sea and Sulu Sea areas, from the newly born Sangihe arc (low-alumina andesite series) and from the Sulu, Zamboanga, and Negros arcs (high-alumina basalt series and high-K andesite series). In the late Pliocene and the early Pleistocene, renewal of activity affects the Sangihe-Cotobato arc as well as the Sulu and Negros arcs (same magmatic distinctions). The last volcanic pulse took place in the late Pleistocene with revival of all the present arc systems.

INTRODUCTION

Volcaniclastic material was recovered in Oligocene to Quaternary sediments of the Celebes Sea and Sulu Sea Basins during Leg 124 (Fig. 1). It consists of dispersed glass shards and magmatic minerals, discrete ash layers, and reworked pyroclastic and hyaloclastic tuffs (nomenclature, grade size limits and terms according to Fisher, 1961, 1966, pers. comm., and Fisher and Schmincke, 1984). The tephrostratigraphic record relates the history of volcanic activity surrounding the basins: north Sulawesi and Sangihe arcs, old and present Philippines arc systems (Manila, Cotobato, and Sulu arcs). We examine the petrographic and chemical compositions of this volcaniclastic material, mainly related to explosive activity, in an attempt to determine their magmatic origin and evolution.

ASH AT LEG 124 SITES

Two sites were drilled in the Celebes Sea Basin (767 and 770) and three in the Sulu Sea Basin (768, 769, and 771). The tephrochronologic investigations are presented in Pubellier et al., (this volume).

Celebes Sea

Sites 767 and 770 are located in the northeastern Celebes Sea. Numerous volcanoes surround the sites at distances of 200 to 400 km. They are located in the North Sulawesi arc, Sangihe arc, central Mindanao and Cotobato arcs, and Sulu ridge.

Important Plinian activity of rhyolitic composition is registered from 2.5 Ma to the Holocene. A second pulse of

volcanism occurred between 8 and 4 Ma and is characterized by more mafic products (dacite and andesite). The Miocene strata, poor in glass fragments, include some altered andesitic microscoria and pyroclastic minerals (feldspars, pyroxenes, and amphiboles). Variably altered andesitic-to-rhyolitic glasses occur within Oligocene sediments. They are abundant in early Oligocene beds and dispersed in late Oligocene beds, indicating distant activity.

Sulu Sea

Site 768 is located in the southeastern part of the Sulu Sea. Site 769 is in the southeast flank of the Cagayan Ridge and Site 771 is on the Cagayan Ridge. Active and Quaternary volcanoes are very near these sites, in the Cagayan Ridge, and 150 to 300 km-distant, in the Sulu Ridge, and on the Panay and Negros Islands.

Sites 768 and 769 registered volcanic activity since late early Miocene time. Site 771 was devoted to basement objectives. Numerous dacitic to rhyolitic ash layers are interbedded in late Miocene to Holocene sediments. They indicate important proximal explosive activity. More mafic and andesitic products are encountered in early Pleistocene beds. Late early to middle upper Miocene strata are poor in volcanic material, which consists of dispersed rhyolitic glass shards, magmatic minerals, and scarce andesitic to dacitic altered glass fragments. Important activity took place in the late early Miocene with the deposition of thick vitric and lithic tuff and lapilli-tuff of pyroclastic (Site 768) or hyaloclastic (Site 769) origin. These tuffs overlie the lava flows of the basement from which they are separated only by a few meters of brown clay.

PETROCHEMICAL STUDY

Sampling

A total of 70 samples were selected to obtain a representative chronological record of the magmatic characteristics in glass and mineral composition of the different areas. Table 1 gives the location and the significant petrographical, chemical, and mineralogical features of the samples. Volcaniclastic

¹ Rangin, C., Silver, E. A., von Breymann, M. T., et al., 1990. *Proc. ODP, Sci. Results*, 124:College Station, TX (Ocean Drilling Program).

² Laboratoire de Géotectonique et Pétrologie, Université d'Orléans, 45067 Orleans, France.

³ Laboratoire de Géotectonique, Université Pierre et Marie Curie, 75252 Paris, France.

⁴ Istituto di Scienze della Terra, Università di Udine, Italy.

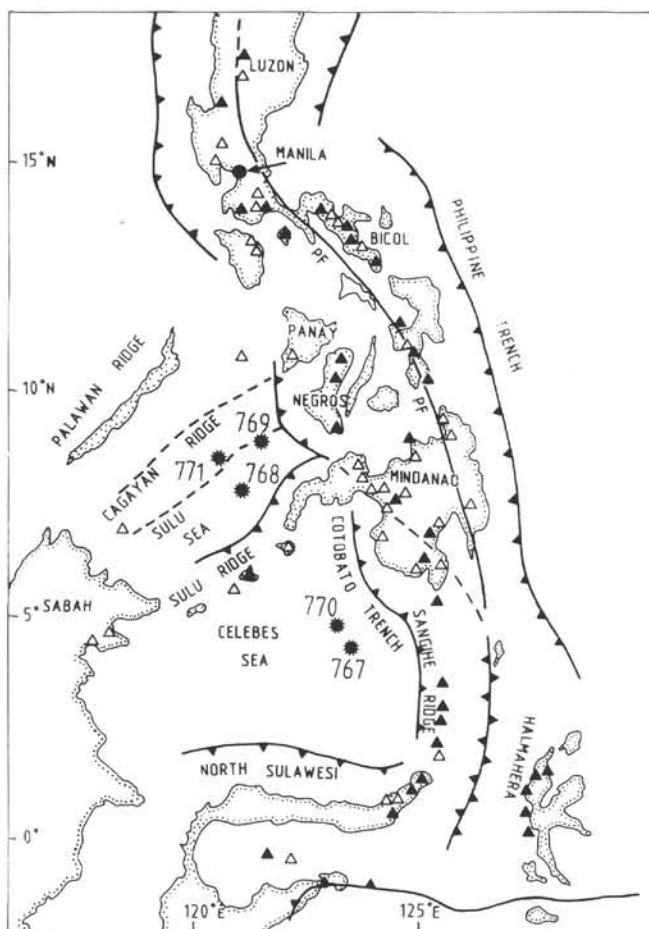


Figure 1. Geographic and structural setting of Leg 124. Sites 767, 768, 769, 770, and 771. PF, Philippine Fault. Full triangles, Holocene volcanoes; open triangles, Pliocene-Pleistocene volcanoes.

material corresponds to vitric ashes and to magmatic minerals; it was investigated in 26 ash layers (glass > 60%), 12 ash-bearing beds (10% < glass < 60%), 4 tuffs, and 28 crystal-rich beds. This selected material is from fallout deposits.

Chronostratigraphic determinations give the following age groups from present to old: 1, Holocene-late Pleistocene; 2, middle Pleistocene; 3, early Pleistocene; 4, late Pliocene; 5, early Pliocene; 6, late Miocene; 7, middle Miocene; 8, early Miocene; 9, late Oligocene; 10, early Oligocene.

We observe three kinds of ash deposits:

1. H (homogeneous), discrete ash layers from single eruptions with weak mixing, good sorting and single mineral and chemical composition. That corresponds to type I of Huang (1980).

2. T (heterogeneous), mixed ashes from frequent, close-spaced eruptions and/or synchronous eruptions from multiple chambers (magma mingling). That is type II of Huang (1980).

3. D, dispersed ashes in sediments.

The shape of glass fragments is given in order of abundance. Sizes and morphologies of fragments indicate Plinian eruptions (shards, tubular micropumices, bubble-wall, or U and Y-reticulite fragments), or sub-Plinian to Vulcanian eruptions (shards and microscorias).

Analytical Method

We used an electron-probe microanalyzer (EPMA) (Camembax C-U-B, Orleans, France), at an accelerating voltage of 15 kV, a specimen current of 5 nA, a beam diameter of 1 to 5 μm , and a time count of 10 s. Specimen current and time count are as low as possible for spot analyses of glass. A large defocused beam is generally required for that kind of material, but it does not allow one to analyze tiny fragments or heterogeneous glasses. Frequently, the width of shards and reticulite fragments is less than 10 μm , and glasses contain microcrysts of tridymite, feldspar, and oxides.

The analytical conditions bring about about Na and K evaporation, a loss (shifting) of Al and some other elements, and, consequently, an Si-enrichment. Measurements were corrected by systematic adjusting with reference to high-quality synthetic glasses of known composition.

Significance of Glass Analyses

The total amount of oxide components range from 86% to 98%. The deficit comes from the initial volatile component, and from hydration and post-depositional alteration in seawater. The initial volatile component (magmatic volatile content and contamination during volcanic processes) may be as high as 5% in dacitic to rhyolitic glasses. Concurrently, hydration occurs rapidly to reach a saturation point of 4% to 5%. Beyond this point, secondary clay minerals develop in the glass giving an optically visible alteration (Pouclet et al. 1985, 1990).

To test the possible effect of hydration on the chemical composition, we calculated the correlation coefficients between oxides content and the analytical deficit (total of oxides) in all the felsic glass analyses (when no alteration was detected). There is a negative correlation for SiO_2 (-0.689). But positive correlations affect, in decreasing order, Na_2O (+0.846), Al_2O_3 (+0.790), Fe_2O_3 total and MnO (+0.773), TiO_2 (+0.758), MgO (+0.711), CaO (+0.688), and K_2O (+0.517). This is due to the relative leaching of these elements during hydration.

Then we calculated, for the whole population, the correlation coefficients between SiO_2 and the oxides: TiO_2 , -0.843; Al_2O_3 , -0.858; Fe_2O_3 total and MnO , -0.880; MgO , -0.892; CaO , -0.931; Na_2O , -0.439; K_2O , -0.154. All the oxides except K_2O and, to a lesser extent, Na_2O , strongly decrease as SiO_2 increases, from basic to acidic composition (differentiation effect). Taking into account this effect and the hydration effect, we corrected the raw data by adjusting the SiO_2 values, compared to the other elements, and we calculated the analyses to 100% (water-free) to obtain an internally consistent analytical population (Table 2). However, in the case of high hydration (7%–9%) and possible smectite formation, the correction is inadequate. Important alkali loss is the cause of high normative corundum content (late to middle Miocene glasses of Site 768).

Chemical Composition of Glasses

Analytical Data

Volcanic glass was analyzed in 45 samples (Table 1). Usually, an average of 6 to 12 analyses per sample (range, 1 to 20 analyses) is done, depending the amount, homogeneity, and freshness of vitric fragments. In addition, approximate compositions were estimated in 7 samples for scarce and highly altered glass fragments. Silica content varies from 53% to 79%. Glasses are only acidic (SiO_2 > 68%) in 31 samples, and only basic or basic to intermediate (53% < SiO_2 < 68%) in 12 samples: they are both basic and acidic in 2 samples. Most of the ash layers are homogeneous.

Normative compositions are strongly oversaturated ($20 < \text{quartz} < 40$) and aluminous ($1 < \text{corundum} < 3$) for acidic glasses, oversaturated ($4 < \text{quartz} < 20$) for intermediate glasses, and saturated ($0 < \text{quartz} < 4$) to undersaturated ($0 < \text{olivine} < 8$) for basic glasses, some of them having normative nepheline. Very high normative corundum-rich glasses are discarded. Oversaturated mafic compositions are encountered in all the sites. Undersaturated mafic compositions characterize the Sulu and Cagayan Sites. Table 2 presents a selection of analyses, in chronologic order, for the three areas: Celebes, Sulu, and Cagayan.

On-board major- and minor-element X-ray fluorescence (XRF) analyses were performed on 16 volcaniclastic samples (Rangin, Silver, von Breymann, et al., 1990). Analyses of raw or incompletely washed samples concern fresh or altered vitric ashes, fallout, and detrital or authigenic minerals, as well as biogenic material. Because of an insufficient amount of material, few samples were purified. Consequently, uncertainty remains about magmatic compositions. There are discrepancies between microprobe glass analyses (EPMA) and whole-sample XRF analyses. For dacite ashes, XRF measurements give lower Si-content and higher Fe, Mg, Ca, and V-contents, possibly due to the presence of plagioclase, pyroxene, and/or amphibole in the raw samples. For rhyolite ashes, XRF measurements give higher Al, Fe, Mg, Ca, K, and Ba-contents, possibly due to the presence of pyroxene, biotite, and alkaline feldspar. Only one ash was sufficiently clean for analysis of rare-earth elements (REE) by emission spectrometry ICP method: Sample 7 (124-767B-3H-1, 88–90 cm). This is a medium-K rhyolite from mid-Pleistocene strata (Table 3). Low REE abundances and slight light REE-enrichment (chondrite normalized La/Yb = 2.80) are consistent with evolved products from island-arc suites. A moderately negative Eu anomaly may have resulted from feldspar fractionation.

Variation Diagrams

Analyses were plotted on SiO_2 vs. oxides variation diagrams (Fig. 2). TiO_2 , total Fe_2O_3 , MgO , and CaO decrease with increasing SiO_2 . Al_2O_3 shows no variations, or weakly increases from 53% to 68% SiO_2 and then decreases. In the same silica range, alkalies increase and then decrease. Important chemical variations affect mafic and intermediate glass analyses, especially for the alumina and alkalies content. This is partly due to heterogeneity of glasses including numerous feldspar microcrysts. However, taking into account the averaged calculations, mafic glasses are classified into two groups: *Al-rich group* ($\text{Al}_2\text{O}_3 > 16\%$), occurring at all the sites, and *Al-poor group* ($\text{Al}_2\text{O}_3 < 16\%$), at Sites 767 and 769. On the $\text{Na}_2\text{O}-\text{K}_2\text{O}-\text{CaO}$ diagram (Fig. 3), the alkali composition is sodic; but some Celebes and Sulu seas volcanics show a potassic trend.

As a whole, considering the Al, Na, K, and Ti contents and the lack of Fe-enrichment (A-F-M diagram, Fig. 4), chemical compositions of glasses may be related to more-or-less potassic calc-alkaline magmatic series. For the $\text{SiO}_2-\text{K}_2\text{O}$ diagram (Fig. 2), compositions belong to the *medium-potassic andesite series* and to the *high-potassic andesite (shoshonite) series*.

Chemical Composition of Minerals

Pyroclastic crystals and epiclastic detrital grains are generally present in selected samples. They consist of feldspar, pyroxene, amphibole, oxides, biotite, and rare olivine. They have been analyzed when not too altered (Table 4). Table 1 presents summarized data.

Feldspars

Feldspars were found and analyzed in almost all the samples. They exhibit a very large compositional range, from An 93 to An 12 for plagioclases, and to Or 98 for alkaline feldspars. Zonation is rarely observed because fragments are small (e.g., An 76-60 in a crystal from Sample 124-767B-28X-1, 135–138 cm). Associated fragments in a layer, however, commonly show various An-contents and plagioclase-alkaline feldspar pairs. There is a correlation between feldspar An and Or-content and glass petrochemical types: An 93-60 with basaltic andesite, An 75-40 with andesite, An 50-20 and Or 20-60 with dacite, An 40-12 and Or 40-98 with rhyolite. Acidic ash beds may include An-rich plagioclase clasts or detrital grains attributed to magmatic xenocrysts or to erosional products of volcanic terrane.

There are different crystallization trends on the An-Ab-Or diagram (Fig. 5), particularly in the intermediate oligoclase-anorthoclase compositional area. Extent of K-rich plagioclase and of Ca-rich alkaline feldspar solid solutions indicates high (900°C) to low (650°C) temperature of crystallization of intermediate evolved liquids (Barth, 1962; Seck, 1971). There is no evident correlation between Al and K-chemical characters of glasses and the temperature crystallization trends of feldspars. The latter may be controlled first by the magmatic-tectonic setting of volcanoes. Coexisting plagioclases and alkaline feldspars have been found in polymineral fragments, for example in Site 767:

- 1, An60 - Or1.8 and An12 - Or24 (Sample 124-767B-28X-1, 135–138 cm);
- 2, An53 - Or1.6 and An11 - Or55 (Sample 124-767B-7H-4, 71–73 cm);
- 3, An37 - Or3.1 and An1.8 - Or68 (Sample 124-767B-76X-4, 110–112 cm);
- 4, An24 - Or3.1 and An1.6 - Or44 (Sample 124-767C-6R-1, 17–19 cm).

They correspond to *high-temperature crystallization trends* (associations 1 and 2, andesitic-dacitic liquid), and to *low-temperature crystallization trends* (associations 3 and 4, dacitic-rhyolitic liquid).

Pyroxenes

Clinopyroxenes (CPX) and orthopyroxenes (OPX) have been analyzed in 17 samples. CPXs are determined as diopside: En 49-43, Wo 46-37 (Fig. 6). Except for two Al and Fe^{3+} -rich pyroxenes from basaltic andesite ash layers (Samples 124-767B-2H-7, 36–38 cm, and 124-767B-21X-5, 139–141 cm), they have high Si and low Al, Ti, and Na-contents indicating sub-alkaline characters: $\text{SiO}_2 50\%$, $\text{Al}_2\text{O}_3 < 4\%$, $\text{Al}_{IV} < 0.10$, and $\text{Ti} < 0.05$ for six oxygens. They are associated with mafic glasses. Rare detrital grains occur in rhyolitic beds.

OPXs are bronzite to hypersthene: En 77-51, Wo 0.2-7.0. They are associated with acidic glasses and indicate a calc-alkaline signature,

In a lithic fragment from Sample 124-769B-3H-6, 25–27 cm, two pyroxenes coexist with plagioclase An48 and andesitic glass. A CPX-OPX geothermometer (Wells, 1977) indicates 1042°C. This liquidus temperature assigned to plagioclase-liquid equilibrium (Kudo and Weill, 1970; Mathez, 1973) corresponds to an H_2O pressure of 2 kbars, in good agreement with the thermobarometric pattern of an andesitic magma.

Table 1. Leg 124 core location and petrographic, chemical, and mineralogical features of the tephra samples. Age group and type, see text.

Sample no.	Core, section, interval (cm)	Age group	Lithology % sand-silt-clay	Glass %	Ash type	Volcanic glass medium size range (extra range)	SiO ₂ range	Alk. feldspar An/Or range	Mineralogy Plagioclase An/Or range	Pyroxene En/Wo range	Amphibole name	others & notes	
770B													
1	1R-2, 19–21	1	70-30-0	65	T sh, bw	50–150 (200)	77.07–77.95	42-38/1.2-1.6			Mg-Hb		
2	1R-3, 75–77	1	80-20-0	60	H sh, bw	50–150	77.66–78.13	36/2.0			Mg-Hb		
767A													
3	1H-1, 74–76	1	20-80-0	30	D sh	30–80	77.76–79.63		34/2.0		Mg-Hb		
4	1H-3, 68–70	1	90-10-0	90	T sh, bw	60–250 (400)	73.80–75.33						
767B													
5	1H-3, 77–79	1	60-40-0	85	G sh, bw, mp	30–250 (350)	73.06–76.15		83-60/0.4-1.4	46-43/39-37	Mg-Hb	Ol (Fo 79.5)	
6	2H-7, 36–38	2	80-20-0	40	T bw, sh, mp	50–150	58.49–67.13		21/11	40/41			
7	3H-1, 88–90	2	80-20-0	90	H bw, sh, mp	60–200	75.63–76.56						
8	7H-4, 71–73	3	80-20-0	90	H sh, bw	60–200	74.12–77.51	11/55	53-35/1.6-4.3	66-65/2.7-2.2	Mb-Hb	Mt (6.5–9.5)	
9	8H-4, 21–23	3	80-20-0	65	T bw, sh, mp	40–120 (600)	77.11–78.32	0/98	35-30/0.7-1.3	66-63/2.1-2.3	Mg-Hb	Ep	
10	9H-3, 85–87	3	70-30-0	65	T bw, sh, mp	40–110 (250)	77.09–79.14	5/45	37-30/0.7-1.1	64/1.9	Mg-Hb		
11	10H-6, 83–85	3	70-30-0	85	H sh, bw, mp	30–120 (180)	77.97–79.15		42-31/2.3-3.2	70/0.2			
12	10X-CC, 12–14	3	10-60-30	60	H sh, bw	25–40 (100)	75.81–77.06						
13	21X-5, 139–141	4–5	20-80-0	60	T sh	30–50 (180)	59.09–64.54	4/41	93-75/0.3-1.0	49-45/43-41	P-Hb	alt. Mt	
14	24X-3, 90–92	5	30-70-0	15	D sh, mp	30–80 (160)	59.56–71.27		73-50/1.0-2.6		P-Hb		
15	26X-5, 57–59	5	70-30-10	80	T bw, sh	50–120	76.96–78.01		34-31/2.4-3.0			alt. Mt	
16	28X-1, 135–138	5	40-60-0	tr	D gr	30–50	(61)	12-0/24-90	71-22/1.3-9.2	44/40	Mg-Hb	Mt (8.8–9.2), smect Bi (61–58; 3.9–3.5)	
17	30X-3, 54–56	5	90-10-0	n				0.3/71	23/5.1-5.3				
18	32X-3, 97–99	5	40-30-30	tr	D gr	30–50	(59)		47-36/1.0-2.2				
19	40X-1, 18–20	6	20-40-40	n				1.2/74	42-40/2.4-2.6		Mg-Hb		
20	43X-2, 21–23	6	10-40-50	n					45/1.2				
21	60X-7, 19–20	7	0-40-60	n				0/85	11/4.4				
22	67X-5, 17–18	7–8	10-70-20	n				0/86	80/0.9		Qtz, Ab		
23	73X-7, 22–24	8	0-10-90	n					46/1.3		Illite		
24	76X-4, 110–112	8–9	30-60-10	n				2-0/68-97	37-13/0.8-6.1		Qtz		
767C													
25	6R-1, 17–19	9	50-40-10	tr	D gr	80–150	77.58	2-0/44-97	46-24/2.2-3.1				
26	6R-2, 147–149	9	10-80-10	tr	D gr	20–100	(62)	0.7/70			Mt (9.5), IIm (28.8)		
27	7R-CC, 8–10	10	10-80-10	n				0.7/70			Mt (11.2), alt. glass		
28	8R-1, 136–138	10	30-70-10	30	D gr	10–130	75.84–76.79		53-42/0.9-4.0			Mt (15.9), alt. glass	
768B													
29	1H-2, 99–101	1	10-80-10	n					11-8/24-30				
30	2H-1, 41–43	1	80-20-0	70	T sh, bw	50–200 (500)	77.15–77.74						
31	3H-1, 54–56	1–2	50-40-10	10	D sh	15–80 (120)	77.57–77.93	0/79	34/2.0			Bi (66–63; 3.4–3.1)	
32	3H-3, 118–121	1–2	60-40-0	60	H sh, bw	30–100	78.11–78.58	12/31	87-41/0.1-1.2		Mg-Hb		
33	4H-2, 148–150	2	60-40-0	60	H bw, sh, mp	40–110	76.14–77.72		40-36/1.9-2.0		Mg-Hb	Mt (5.4)	
34	4H-6, 65–67	2	70-30-0	80	T sc	40–120 (200)	56.55–62.11		88-53/0.3-3.8	43/44	Mg-Hb	Mt (7.1)	
35	4H-7, 45–47	2	80-20-0	85	T bw, sh, mp	50–200 (300)	57.40–67.53		20-14/11-20				
36	4H-7, 82–84	2	80-20-0	80	H sc	50–120	54.51–57.75		85/0.9	42/43		Mt (7.6)	
37	12H-7, 22–24	3	10-30-60	n				1/24	67-39/0.4-3.0		Fe-P-Hb	Bi (71/3.2)	
38	14H-3, 113–115	3–4	0-20-80	5	D gr, sh	30–50	77.62–78.07				Mg-Hb		
39	15H-2, 29–31	4	60-40-0	8	D sh, .g	50–200	73.60–74.36	10/38	48-44/0.5-0.9		Mg-Hb		
40	16H-2, 49–51	4	10-30-60	n					38-15/0.9-8				
41	16H-3, 118–120	4	50-50-0	tr	D gr	30–80	79.25	6/42	33-27/1.8-2.8		Mg-Hb	Mt (4.6), IIm (26.5)	
42	18H-4, 106–108	5	50-50-0	10	D sh, gr	30–100	(63)	8/56	42/2.5		Mg-Hb	alt. Bi	
43	22H-1, 72–73	5–6	60-30-10	tr	D gr, sh	40–100	78.01–78.58		53-34/0.5-2.9		Mg-Hb	alt. glass	
44	22H-5, 104–105	5–6	30-40-30	n				1.6-0.2/59-83	41-29/3.5-7.5		Mg-Hb	alt. glass	
45	23H-3, 101–102	6	30-50-20	tr	D sh, g	50–100	77.45–77.99		40-39/1.0-1.3	65/3.4	Mb-Hb	IIm (41.7)	
46	28X-3, 91–93	6	60-40-0	n				42-39/1.0-1.3			Mg-Hb	alt. glass	

Table 1 (continued).

Sample no.	Core, section, interval (cm)	Age group	Lithology %			Glass %	Ash type	type	Volcanic glass medium size range (extra range)	SiO ₂ range	Mineralogy				Amphibole name	others & notes
			sand-silt-clay	tr	n						An/Or range	Plagioclase An/Or range	Pyroxene En/Wo range	Amphibole name		
47	29X-4, 49–51	6	10-30-60	tr	D	sh			80–90 (300)	77.68–78.81	5/60	51-45/0.5-2.4			Mg-Hb	
48	35X-1, 117–119	6	20-30-50	n						0/97	54-20/0.7-6.6			Ts-Mg-Hb	alt. glass	
768C																
49	31R-4, 61–63	7	5-30-65	tr	D	gr			20–70	77.61	0.1/96	62/1.8				
50	32R-1, 144–146	7	5-30-65	tr	T	sh, bw, mp			80–160 (250)	77.87–78.64		43-39/2.8-3.9				Qtz, Ilm (47.3)
51	32R-2, 61–63	7	70-30-0	95	T	sh, bw			50–250 (300)	76.25–78.80		50/2				
52	39R-3, 62–65	7	20-70-10	10	D	gr, sh			20–70	67.95	0/94					alt. glass
53	39R-4, 72–74	7	20-70-10	15	D	gr, sh			25–100	73.51–74.73	0.4/79	64-46/1.5-2.2				alt. Bi
54	52R-4, 133–135	8		70	tuff					0.2/90	80-35/0.6-5.9	46-43/46-40		Mg-Hb		
55	52R-6, 51–53	8		60	tuff						64/2					
56	72R-1, 30–32	8	20-70-10	40	tuff	sh			30–60	(70)					alt. glass	
57	72R-1, 55–58	8	20-70-10	30	tuff	sh, gr			30–70	(70)	7-2/63-65				alt. glass	
769A																
58	3H-4, 102–103	2	70-30-0	70	H	sc, bw			100–160	54.19–56.65						
59	4H-4, 146–147	2	70-30-3	80	H	sc, bw			60–250	53.82–56.26		64-55/1.3-2.5				
60	5H-5, 60–62	2	50-50-0	30	D	sh			50–180	61.59–66.44		58-18/1.1-17.7			Mg-Hb	Mt (3.2–4.3)
769B																
61	2H-7, 28–30	1	60-40-0	40	D	sh			30–100 (200)	76.47–78.36		35-28/1.9-2.3				
62	3H-6, 25–27	2	90-10-0	90	T	bw, mp, sh			100–250	56.08–66.34		67-26/1.6-7.2	77/1 + 43/39			Mt (7.8)
63	4H-1, 53–55	2	70-30-0	70	T	bw, sc, sh			50–250	55.67–58.20		83/0.4				
64	5H-4, 82–84	2	40-40-20	30	D	sh, bw			25–150	55.47–74.00		71/0.7	44/42		Mg-Hb	
65	9H-7, 29–31	3	95-5-0	95	H	bw, sh			100–400	74.73–75.71		52/0.9	74-73/2.1-7.0			
66	10H-5, 102–104	3	80-20-0	70	T	sh, sc			50–180	59.83–65.30		41/2.6				
67	12H-2, 4–6	3–4	90-10-0	70	T	sh, mp, sc			100–300	56.14–67.28	0/98	30/5.1				
68	30X-2, 125–127	7	20-50-30	n						1.1/58-60	45/0.4			Mg-Hb	Mt (8.2)	
69	30X-cc, 37–39	7	50-40-10	n							62/1.0				Mt (7.3)	
769C																
70	2R-6, 7–9	7	80-20-0	40	D	sh, mp			30–200 (300)	(65)	0/98		43/42	Mg-Hb	smect	

Abbreviations: tr, trace; n, none; sh, shards, bw, bubble-wall fragments; mp, micropumices; gr, grains; sc, microscoria. Size of glass in μm . Mg-Hb, Mg-hornblende; P-Hb, pargasitic hornblende; Ts-Mg-Hb, tschermakitic or Mg-hornblende; Ab, albite; alt, altered; Bi, biotite ($\text{Mg}/\text{Mg} + \text{Fe}^{2+} + \text{Mn}\%$, $\text{TiO}_2\%$); Ep, epidote; Ilm, ilmenite ($\text{TiO}_2\%$); Mt, magnetite ($\text{TiO}_2\%$); Ol, olivine (Forsterite%); Qtz, quartz; smect, smectite.

Table 2. Chemical analyses and norms of glasses. Total Fe as Fe₂O₃: calculated FeO/FeO + Fe₂O₃ = 0.85 for norm calculation.

	A									
	1	2	3	4	5	6.1	6.2	7	8	9
SiO ₂	77.41	77.91	78.55	74.50	74.56	59.12	67.00	76.11	75.54	77.70
TiO ₂	0.13	0.07	0.09	0.36	0.32	0.86	0.40	0.24	0.18	0.07
Al ₂ O ₃	12.94	12.88	12.55	14.03	13.82	17.61	16.92	13.45	13.72	13.95
Fe ₂ O ₃	1.03	0.88	0.94	1.75	1.72	6.65	3.43	1.63	1.38	0.95
FeO	nd									
MnO	0.07	0.10	0.13	0.05	0.15	0.18	0.20	0.10	0.17	0.08
MgO	0.22	0.25	0.22	0.39	0.39	2.03	0.50	0.30	0.25	0.27
CaO	1.12	1.11	0.98	1.36	1.31	4.81	1.23	1.47	0.98	1.34
Na ₂ O	3.96	3.80	3.24	4.12	4.26	4.87	5.07	3.80	3.94	3.60
K ₂ O	3.12	3.00	3.30	3.43	3.46	3.87	5.25	2.90	3.83	2.04
TOTAL	100.00	100.00	100.00	100.00	100.00	100.00	100.00	100.00	100.00	100.00
IL	0.25	0.13	0.18	0.69	0.61	1.72	0.78	0.46	0.34	0.13
MT	0.22	0.19	0.20	0.38	0.38	1.53	0.77	0.36	0.30	0.20
OR	18.43	17.66	19.34	20.37	20.65	24.07	31.84	17.15	22.66	11.77
AB	33.50	32.03	27.17	35.06	36.42	43.38	44.05	32.20	33.33	29.76
AN	5.56	5.49	4.82	6.79	5.44	15.54	6.25	7.30	4.88	6.49
DI	nd	nd	nd	nd	nd	7.99	nd	nd	nd	nd
HY	0.83	0.86	0.85	1.30	1.40	4.49	2.44	1.21	1.09	0.90
C	2.03	2.72	3.71	2.13	1.39	nd	1.36	2.78	2.64	6.62
Q	39.19	40.92	43.74	33.28	32.60	1.29	12.51	38.55	34.76	44.13
TL	100.00	100.00	100.00	100.00	100.00	100.00	100.00	100.00	100.00	100.00
	10	11	12	13	14.1	14.2	14.3	15	25	28
SiO ₂	77.73	78.53	76.58	61.39	63.24	66.25	70.42	77.39	77.58	76.21
TiO ₂	0.09	0.12	0.15	0.68	0.85	0.64	0.88	0.09	0.05	0.01
Al ₂ O ₃	13.61	12.34	13.52	16.08	14.72	15.51	14.00	13.09	13.39	14.34
Fe ₂ O ₃	1.02	0.86	1.08	6.32	9.02	5.51	4.78	1.05	0.40	0.16
FeO	nd									
MnO	0.13	0.13	0.07	0.16	0.35	0.32	0.04	0.08	0.10	0.09
MgO	0.22	0.13	0.15	2.30	1.55	1.07	0.27	0.18	0.03	0.18
CaO	1.21	0.84	1.00	3.66	3.97	2.69	1.70	1.00	1.93	2.27
Na ₂ O	3.49	3.31	3.25	4.48	3.66	4.23	3.67	3.15	4.02	3.73
K ₂ O	2.50	3.74	4.20	4.92	2.63	3.79	4.24	3.97	2.49	3.02
TOTAL	100.00	100.00	100.00	100.00	100.00	100.00	100.00	100.00	100.00	100.00
IL	0.17	0.23	0.28	1.37	1.77	1.29	1.73	0.17	0.10	0.02
MT	0.22	0.19	0.23	1.45	2.14	1.27	1.08	0.23	0.09	0.03
OR	14.50	21.99	24.60	30.66	16.91	23.59	25.89	23.28	14.67	17.74
AB	28.99	27.87	27.27	39.94	33.69	37.72	32.10	26.45	34.00	31.40
AN	5.89	4.15	4.92	9.72	17.34	12.83	8.72	4.92	9.57	11.21
DI	nd	nd	nd	7.90	3.31	1.03	nd	nd	nd	nd
HY	0.87	0.64	0.72	4.89	6.41	4.23	2.32	0.80	0.28	0.43
C	5.82	2.63	3.59	nd	nd	nd	0.58	3.56	1.13	1.61
Q	43.54	42.30	38.38	4.06	18.43	18.03	27.57	40.59	40.16	37.55
TL	100.00	100.00	100.00	100.00	100.00	100.00	100.00	100.00	100.00	100.00
	30	31	32	33	34	35.1	35.2	35.3	36	38
SiO ₂	77.57	77.72	78.36	76.69	58.74	57.40	63.29	66.92	55.92	77.76
TiO ₂	0.10	0.06	0.19	0.22	0.84	0.89	0.66	0.37	0.96	0.24
Al ₂ O ₃	13.08	12.90	12.15	12.98	17.44	17.15	17.43	17.14	16.41	12.18
Fe ₂ O ₃	0.74	0.22	1.28	1.02	6.75	8.77	4.08	2.59	9.35	1.66
FeO	nd									
MnO	0.11	0.19	0.07	0.07	0.15	0.11	0.15	0.13	0.19	0.12
MgO	0.18	0.05	0.20	0.23	2.32	2.52	1.19	0.39	3.26	0.23
CaO	0.92	1.02	1.24	1.12	4.91	5.73	2.78	1.10	6.36	1.34
Na ₂ O	3.87	3.93	3.61	3.89	5.12	4.05	5.59	5.48	4.21	3.80
K ₂ O	3.43	3.89	2.90	3.78	3.71	3.38	4.83	5.88	3.34	2.67
TOTAL	100.00	100.00	100.00	100.00	100.00	100.00	100.00	100.00	100.00	100.00
IL	0.19	0.12	0.35	0.42	1.67	1.82	1.29	0.72	1.90	0.46
MT	0.16	0.05	0.28	0.22	1.54	2.06	0.92	0.58	2.13	0.37
OR	20.15	22.97	17.20	22.43	22.90	21.48	29.40	35.54	20.61	15.92
AB	32.57	33.29	30.67	33.10	45.28	36.87	48.73	47.44	37.24	32.45
AN	4.54	5.08	6.19	5.57	14.24	20.05	8.45	4.91	16.70	6.71
DI	nd	nd	nd	nd	9.38	8.76	4.80	0.55	13.61	nd
HY	0.67	0.29	.88	0.78	3.89	6.34	2.54	1.67	3.64	1.13
OL	nd	nd	nd	nd	1.10	nd	nd	nd	4.17	nd
C	2.64	0.73	1.62	0.91	nd	nd	nd	nd	nd	1.22
Q	39.08	37.48	42.81	36.57	nd	2.63	3.86	8.60	nd	41.76
TL	100.00	100.00	100.00	100.00	100.00	100.00	100.00	100.00	100.00	100.00
	39	41	43	45	47	49	50	51	52	53
SiO ₂	74.02	79.25	78.29	77.80	78.22	77.61	78.23	77.42	67.95	74.06
TiO ₂	0.25	0.10	0.13	0.20	0.17	0.24	0.10	0.13	0.11	0.08

Table 2 (continued).

	Al ₂ O ₃	13.74	11.39	14.01	14.40	14.18	14.11	14.23	13.97	18.79	16.19
	Fe ₂ O ₃	1.83	0.32	1.40	1.33	1.56	1.53	1.38	1.41	0.53	0.13
	FeO	nd									
	MnO	0.13	0.13	0.06	0.10	0.05	0.22	0.06	0.12	0.05	0.06
	MgO	0.48	0.19	0.15	0.13	0.17	0.10	0.11	0.14	0.29	0.28
	CaO	1.50	0.72	0.97	0.98	1.04	0.85	0.95	1.00	3.82	2.16
	Na ₂ O	4.67	3.62	2.68	2.78	2.39	2.73	2.78	3.38	3.53	3.30
	K ₂ O	3.37	4.29	2.31	2.28	2.22	2.61	2.16	2.43	4.93	3.74
TOTAL		100.00	100.00	100.00	100.00	100.00	100.00	100.00	100.00	100.00	100.00
IL	0.49	0.19	0.24	0.36	0.31	0.44	.18	0.24	0.21	.15	
MT	0.41	.07	0.29	0.28	0.33	0.32	0.29	0.30	0.12	0.03	
OR	20.28	25.36	13.11	12.90	12.54	14.84	12.22	13.98	29.11	21.56	
AB	40.22	30.65	21.78	22.52	19.33	22.24	22.54	27.86	29.85	27.25	
AN	6.66	2.19	4.62	4.65	4.93	4.06	4.52	4.83	18.94	10.46	
DI	0.76	1.17	nd								
HY	1.44	0.20	0.85	0.77	0.92	0.88	0.80	0.89	0.70	0.50	
OL	nd	nd	nd	nd	nd	nd	nd	nd	nd	nd	
C	nd	nd	10.27	10.69	11.40	10.12	10.73	7.73	1.40	5.44	
Q	29.74	40.17	48.84	47.83	50.25	47.10	48.73	44.16	19.67	34.62	
TL	100.00	100.00	100.00	100.00	100.00	100.00	100.00	100.00	100.00	100.00	
		C									
		61	62.1	62.2	58	63	59	64.1	64.2	64.3	60
	SiO ₂	77.94	56.46	66.26	55.05	57.32	55.00	55.47	64.13	73.99	66.44
	TiO ₂	0.08	1.07	0.34	0.99	0.82	0.99	1.18	1.00	0.14	0.96
	Al ₂ O ₃	12.58	16.52	17.78	16.95	16.41	17.83	14.17	14.65	14.38	16.31
	Fe ₂ O ₃	0.83	8.67	2.55	9.23	7.73	7.64	11.22	6.16	1.36	3.29
	FeO	nd									
	MnO	0.09	0.10	0.02	0.17	0.15	0.11	0.19	0.12	0.09	0.23
	MgO	0.15	2.92	0.36	3.13	2.63	3.19	4.68	1.63	0.21	1.49
	CaO	1.12	5.89	1.15	7.16	5.84	6.18	6.65	4.36	1.20	2.28
	Na ₂ O	3.57	5.27	5.65	4.26	4.97	5.20	4.35	4.86	4.13	5.67
	K ₂ O	3.65	3.10	5.89	3.07	4.13	3.87	2.07	3.09	4.50	3.33
TOTAL		100.00	100.00	100.00	100.00	100.00	100.00	100.00	100.00	100.00	100.00
IL	0.14	2.05	0.66	1.91	1.57	1.89	2.44	1.97	0.27	1.88	
MT	0.18	1.90	0.57	2.04	1.70	1.67	2.65	1.39	0.30	0.74	
OR	21.61	18.44	35.58	18.40	24.56	22.88	13.25	18.88	26.79	20.30	
AB	30.23	42.28	48.88	36.58	38.25	31.49	39.87	42.52	35.22	49.44	
AN	5.57	12.35	5.83	18.33	10.34	13.92	14.09	9.34	6.00	9.49	
DI	nd	14.28	nd	14.81	15.74	14.12	18.21	10.83	nd	1.85	
HY	0.66	nd	1.67	0.69	nd	nd	7.90	2.61	0.99	3.24	
OL	nd	7.28	nd	7.24	5.63	7.25	1.60	nd	nd	nd	
NE	nd	1.42	nd	nd	2.21	6.79	nd	nd	nd	nd	
C	1.44	nd	0.04	nd	nd	nd	nd	nd	1.08	nd	
Q	40.17	nd	6.77	nd	nd	nd	nd	12.46	29.36	13.06	
TL	100.00	100.00	100.00	100.00	100.00	100.00	100.00	100.00	100.00	100.00	
		65	66.1	66.2	67.1	67.2					
	SiO ₂	75.27	59.94	64.33	56.14	66.25					
	TiO ₂	0.25	0.86	0.72	1.08	0.53					
	Al ₂ O ₃	13.96	17.33	16.79	17.32	16.75					
	Fe ₂ O ₃	1.37	7.00	4.99	9.10	4.60					
	FeO	nd	nd	nd	nd	nd					
	MnO	0.13	0.28	0.25	0.22	0.01					
	MgO	0.26	2.06	1.49	3.05	0.67					
	CaO	1.12	4.59	3.16	6.04	2.20					
	Na ₂ O	4.05	4.44	4.40	4.51	4.63					
	K ₂ O	3.59	3.50	3.86	2.54	4.38					
TOTAL		100.00	100.00	100.00	100.00	100.00					
IL	0.48	1.74	1.44	2.23	1.04						
MT	0.30	1.63	1.15	2.14	1.04						
OR	21.19	22.03	24.00	16.24	26.83						
AB	34.24	40.03	39.19	41.25	40.64						
AN	5.55	18.14	15.44	21.11	11.34						
DI	nd	5.10	0.89	9.43	nd						
HY	1.03	5.59	4.61	7.27	3.12						
OL	nd	nd	nd	nd	nd						
NE	nd	nd	nd	nd	nd						
C	2.75	nd	nd	nd	0.84						
Q	34.47	5.74	13.28	0.32	15.16						
TL	100.00	100.00	100.00	100.00	100.00						

A. Sites 767, 770. B. Site 768. C. Site 769. Samples are in chronologic order. The table presents one averaged analysis for each homogeneous sample and two or three averaged or representative analyses for heterogeneous samples.

Amphiboles and Biotite

Amphiboles are common minerals in many layers, as pale to dark brown-green fragments. They have been analyzed in 26 samples. All proved to be calcic amphiboles, classified using the Leake (1978) nomenclature (Table 1). Their low Al and Ti-contents are consistent with sub-alkaline characters (Fig. 7). Most of the amphiboles are Mg-hornblendes associated with dacitic and rhyolitic glasses. Pargasitic hornblendes were determined in Site 767 Pliocene strata, in association with andesitic glasses (samples 13, 14). A reddish and high-Mg hornblende has been found in Site 767 Pliocene-Pleistocene strata and associated with feldspar, orthopyroxene, and rare magnetite and epidote, indicating proximity of mafic volcanic terrane. Assuming that amphibole crystallized with all the phases in the lava plus melt, we use the empirical geobarometer of Hammarstrom and Zen (1986): Mg-hornblendes are related to low-pressure crystallization (averaged total Al-content indicates 2.6 ± 3 kb), whereas pargasitic hornblendes correspond to higher pressure crystallization (6.1 ± 3 kb). The Hollister et al. (1987) equation gives the same relative results, respectively 2.5 ± 1.5 kb and 6.5 ± 1.5 kb.

Biotite is less common, as generally oxidized brown flakes. Fresh biotites and Mg-biotites were analyzed in three sam-

Table 3. Minor-element chemical analysis of Sample 124-767B-3H-1,88-90. Inductively coupled plasma emission spectrometry. Elements in parts per million.

La	=	12.80	Ba	=	310
Ce	=	30.54	Be	=	0.8
Nd	=	13.86	Co	=	180
Sm	=	4.30	Cr	=	12
Eu	=	0.76	Cu	=	54
Gd	=	3.87	Ga	=	9
Dy	=	4.39	Ni	=	26
Er	=	2.76	Rb	=	54
Yb	=	3.08	Sc	=	13.3
Lu	=	0.62	Sr	=	149
			V	=	16
			Y	=	35.85
			Zn	=	57
			Zr	=	183

ples. The 100 Mg/Mg+Fe²⁺ ratio ranges from 58% to 66% in "rhyolitic" beds, and to 71% in "mafic" beds, indicating higher PH₂O and fO₂ conditions (Wones and Eugster, 1965). TiO₂ contents vary from 3.2% to 3.9%.

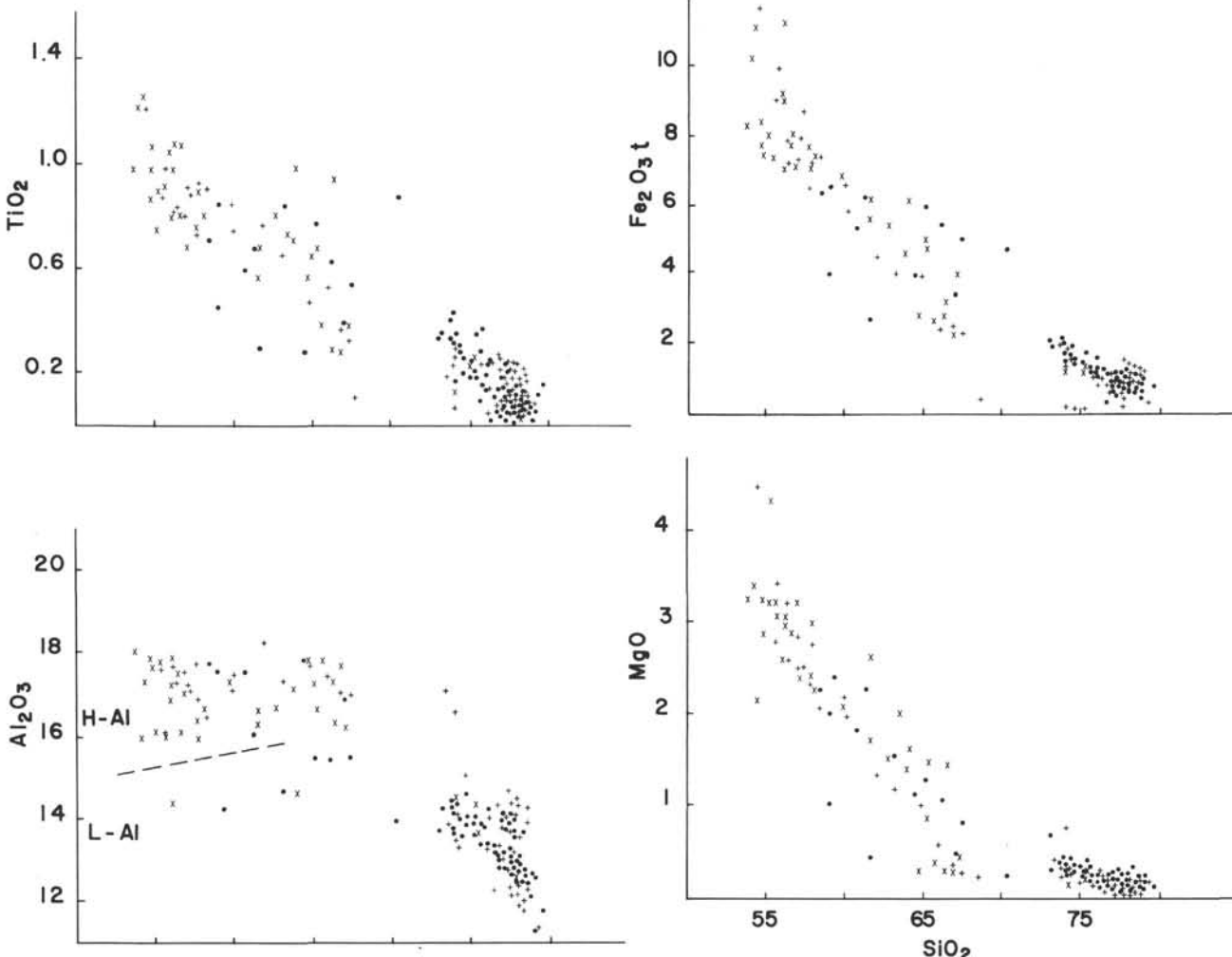


Figure 2. SiO₂ vs. oxides variation diagrams. Solid circles: Sites 767 and 770; cross: Site 768; X: Site 769; L-Al and H-Al, low- and high-alumina compositions. L-K, M-K, and H-K, Low-, medium-, and high-potassiac compositions. B-And, basaltic andesite; And, andesite; DC, dacite; RH, rhyolite.

Oxides

Magnetite occurs as epiclastic and oxidized grains, or as tiny fragments and euhedral pyroclastic crystals that were analyzed in thirteen samples. TiO_2 -contents vary from 3.2% to 9.5% in "rhyolitic" beds, and to 15.2% in "andesitic" beds.

Ilmenite consists of rare fragments that were analyzed in only four samples. They have high TiO_2 content (42%–47%) in "acidic" beds and low TiO_2 content (26%–27%) in "mafic" beds, when coexisting with Ti-rich magnetite and biotite.

Two coexisting iron-titanium oxides were found in two samples. We calculated thermometry and oxygen barometry, using phase recalculations of Stormer (1983) and formulations of Andersen and Lindsley (1988), with the following results:

1. Sample 124-768B-16H-2, 49–51 cm: $T = 842^\circ C$, $\log(10fO_2) = -10.6$. These data are consistent with dacitic liquid composition.
2. Sample 124-767C-6R-1, 17–19 cm: $T = 1035^\circ C$, $\log(10fO_2) = -8.4$. The high temperature and very high oxygen fugacity may be related to volatile-rich andesitic magma.

Miscellaneous Minerals

Detrital epiclastic olivine Fo 79.5 was found in Sample 5 (124-767B-1H-3, 77–79 cm) together with CPX, Ca-plagioclase, and Mg-hornblende, indicating andesitic paragenesis. But coexisting glass shards are rhyolitic in composition. Andesitic scoria are known in slightly older layers at the same

site (124-767B-2H-7, 36–38 cm). Thus, a proximate andesitic source does exist. Detrital epidote pistacite (12.67% Fe_2O_3) was analyzed in Sample 9 (124-767B-8H-4, 21–23 cm), a turbidite rhyolitic ash layer that indicates the proximity of metamorphic terrane.

Petrologic Interpretation and Magmatic Affinities

Chemical variations using all of the glass compositions are depicted in Figure 2. Because several samples contain differentiated basic to acidic glasses together with their minerals, an attempt was made to determine the petrological features that may express magmatic affinities. Distinctive chemical compositions are evidenced with alumina and alkalies vs. silica variations, whereas lime, magnesia, and iron exhibit common decreasing contents from basic to acidic compositions. Selected and averaged samples from Figure 2 are plotted on Figure 8: diagrams of Al_2O_3 , CaO , Na_2O and K_2O vs. SiO_2 . Tie-lines join glass composition types coexisting in ash beds, showing parallel or divergent trends. Dashed lines correspond to probable trends for acidic glasses. Two successive gross variations are distinguishable from andesitic to dacitic glasses, and from dacitic to rhyolitic glasses, with a drastic change at SiO_2 67%–68%. Variations may be due (1) to fractional crystallization, (2) to magma mixing or mingling, (3) to crustal contamination, or (4) to any other secondary process (alkali loss in altered acidic glasses). Either crystal fractionation or crustal contamination may explain the potassium enrichment of some glasses of intermediate silica composition; it is impossible to decipher from the major

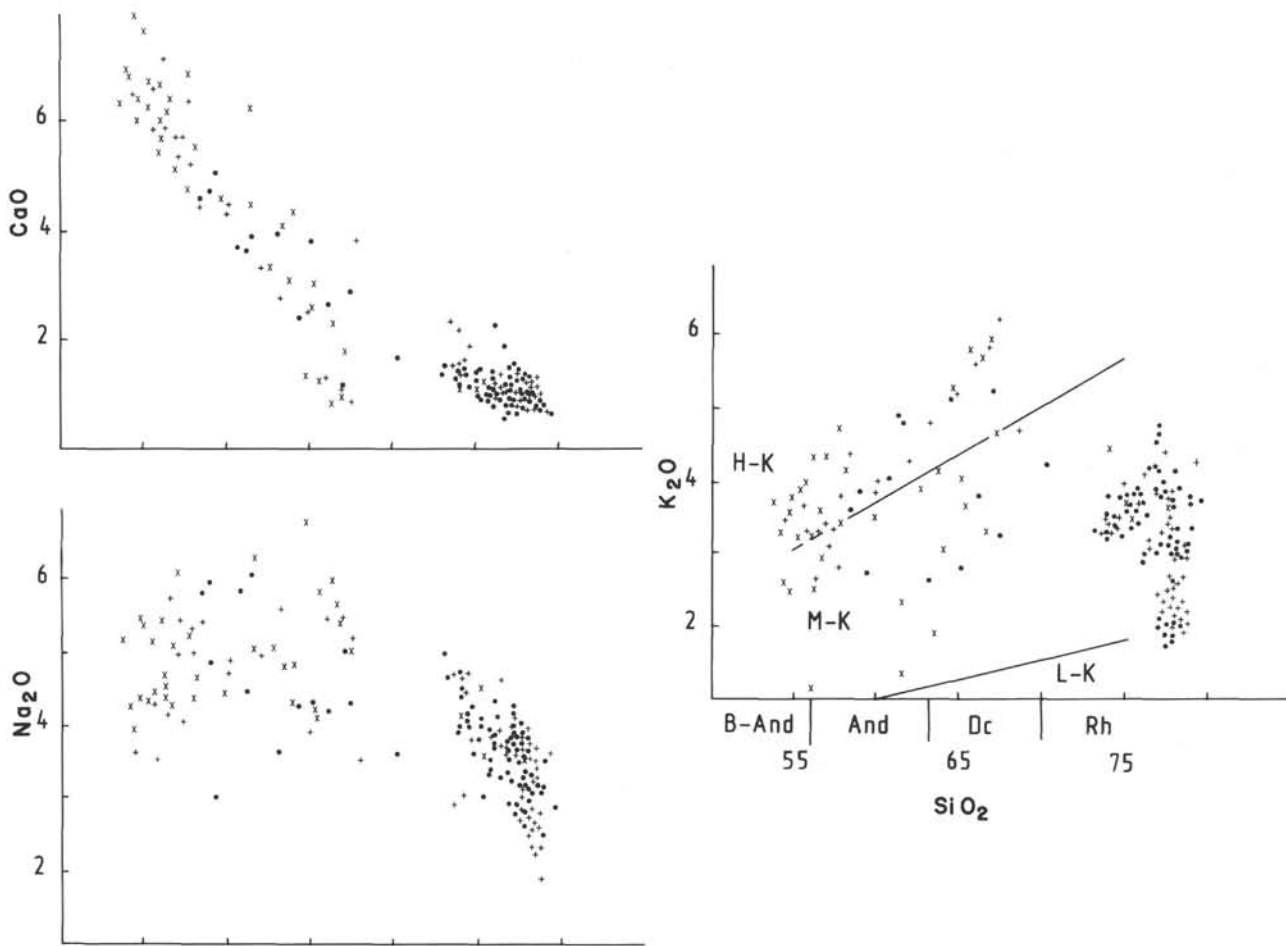


Figure 2 (continued).

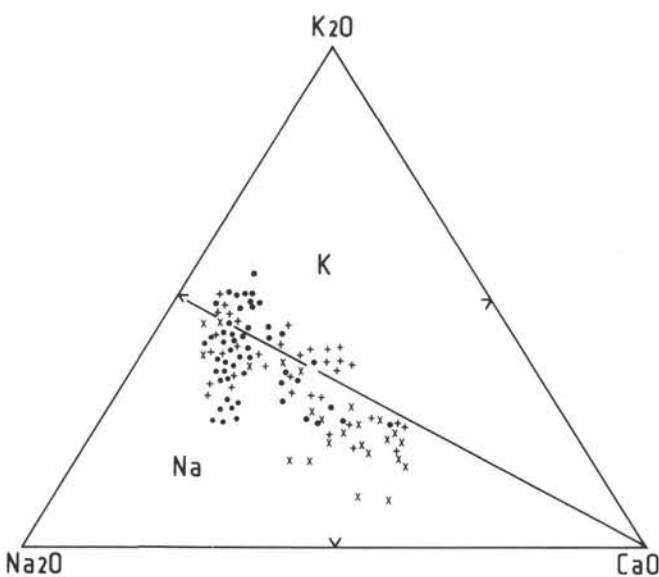


Figure 3. CaO-Na₂O-K₂O diagram; sodic (Na) and potassic (K) fields. Symbols as for Figure 2.

element data. Magmamixing and/or mingling is obvious, considering the very high range of feldspar compositions and the multicompositional ashes; however, in common calc-alkaline volcanoes, this affects the more-or-less differentiated magmas of a cogenetic suites.

By using coexisting mineral analyses and glass compositions, least-square-mass balance calculations can test chemical evolutions in term of fractionation of distinct magmatic series (Wright and Doherty, 1970); Table 5. Samples were selected to represent the different chemical variations in the age groups. When possible, the parent and daughter liquids are coexisting glasses from mixed ash layers having consistent compositional trends. At least they belong to eruptions close in age. Apparently successful calculations (low residuals) are a consequence of the least-squares approach by choosing appropriate phases. We assume that coexisting glasses and minerals in a discrete ash layer originated from a single volcanic system, but we do not know if the glasses are formally parent and daughter liquids. The Table 5 presents a summary of the result (completely documented calculations would give a fallacious impression of accuracy). Trends are numbered according to their increasing slope on an alumina/silica diagram (Fig. 8). As a practical result, we distinguish two fractionation steps and three differentiation trends. This distinction brings an additional guide in ascribing ash deposits to volcanic belts.

The First Fractionation Step

This step, from andesites to dacites, involves clinopyroxenes (Wo 41, En 40-44), titanomagnetites, amphiboles (pargasitic hornblende and Mg-hornblende), Mg-biotites, and plagioclases (An 60-35). These results are only indicative of general evolution. Various calculations can be done, but not with very different solutions. We may distinguish three types of fractionation trend.

Type A

This is a major fractionation of *amphibole*, subordinate plagioclase of the low-temperature trend, and clinopyroxene. This is related to low-pressure crystallization of volatile-rich

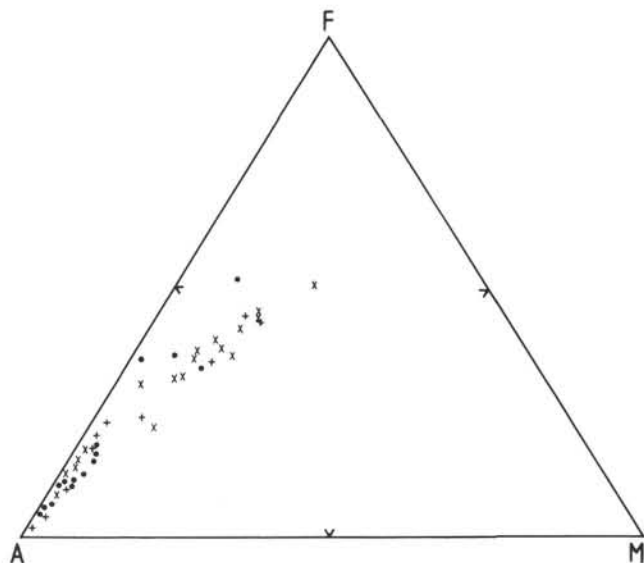


Figure 4. A-F-M diagram (Na₂O + K₂O-total Fe₂O₃-MgO). Averaged analytical data. Symbols as in figure 2.

andesitic magma. These features, and low Al- and alkali-contents (see above) characterize *moderate potassic andesitic series of an island arc*. The type-A magmatic products locate Site 767 in early Pliocene to early Pleistocene strata, and Site 769 in middle to late Pleistocene strata.

Type B

This is a major fractionation of *plagioclase* of the high-temperature trend, amphibole or biotite, and rare clinopyroxene. This is related to high-pressure crystallization of water-undersaturated (PH₂O, 2 kbar - see above) andesitic magma. High-alumina and moderate alkalies contents may correspond to *high-alumina basalt series of an island or continental margin arc*. Type B locates Site 769 in late Pliocene to early Pleistocene strata, and Site 767 in Quaternary strata.

Type C

This is a major fractionation of *clinopyroxene* and *plagioclase* of the high-temperature trend and subordinate amphibole. This is related to high-pressure crystallization of andesitic magma. High alumina and alkalies contents may correspond to *high-K andesite series of an island or continental margin arc*. Type C occurs at Sites 768 and 769, in Quaternary strata.

The Second Fractionation Step

This step, from dacites to rhyolites, concerns titanomagnetites, hornblendes, Mg-biotites, plagioclases (An 45-35), and alkaline feldspars (Or 25-71). Overlapping trends combine removals of clinopyroxenes, titanomagnetites, amphiboles, biotites, plagioclases, and alkaline feldspars. It appears that orthopyroxene is not an intervening phase. OPX only occurs with acidic glasses, except for Sample 62 (124-769B-3H-6, 25-27 cm), where coexisting with CPX. In terms of mineral fractionation, high-K rhyolite compositions result in plagioclases + alkaline feldspars removal, whereas low-K rhyolite compositions suggest heavy fractionation of alkaline feldspars. But in many cases, the K-content of acidic glasses is modified by the alteration. Thus, this last fractionation step is poorly defined.

DISCUSSION

According to the geochemical and petrological interpretations, the volcaniclastic glasses and minerals are assigned to three magmatic series that occurred throughout the two basins: (1) low-alumina and medium-K hornblende andesitic series, (2) high-alumina and medium-K basalt series, and (3) high-alumina and high-K pyroxene andesitic to shoshonitic series.

The first question is: What are the sources of these products? The second question will be: What is the correlation between the Leg 124 tephra composition and the geodynamic evolution of the surrounding areas?

Comparison with Land Volcanics

Various medium- and high-K calc-alkaline suites are known in neighboring volcanic arcs, located in composite transitional crustal environments with oceanic crusts and continental fragments. Their features are summarized as follows. Timing and apparent tectonic control of volcanism are from Wolfe (1981), Rangin et al. (1990), Bellon and Rangin (this volume), and Bellon (this volume). Petrochemical data are interpreted from Divis (1980), Jeseck et al. (1981), Morris et al. (1983), Yuwono (1987), Kudrass et al. (1990), and Bellon and Rangin (this volume).

In the Eastern Philippine magmatic activities occurred from Eocene to early Miocene time in relation with an eastward subduction below the Philippine arc (Eastern Philippines), and since Pliocene, in relation with the westward subduction in the Philippine trench. Lavas consist of pyroxene-hornblende andesites suites of low-alumina and medium-K composition (series A), and also of high-alumina and medium-K basalts (series B).

In the western Philippine (from Zambales to central Mindanao), various volcanic activities are related to complex subductions along the Manila-Sulu trenches, South China Sea and Sulu Sea since the late Miocene. Successive volcanic arcs were accreted (Rangin et al., in press). Some lavas may have low-Al and medium-K composition (series A), but most of the compositions are high-Al and medium-K or high-K, and differentiation trends belong to series B and C defined above. High-K andesites with shoshonitic affinities (series C) seem to locate in transverse structures such as Verde Passage Zone, south of Manila, and central Mindanao.

The South Philippine volcanic zone (South Mindanao and Sangihe arcs) is related to subduction of the Molucca Sea since the late Miocene (Pubellier et al., in press) and of the Celebes Sea in the Cotobato Trench since the early Quaternary. Hornblende andesites are predominant in the northern sector of this zone (series A). High-Al olivine basalts and pyroxene andesites (series B) erupted in the whole zone.

To the south, *the Halmahera Island arc* fringed the Philippine Plate (southern extension of Philippine arc) from Eocene to Miocene time. Since the Pliocene, volcanism is linked to the Molucca Sea subduction toward the east (Hall et al., 1988). It consists of medium-K basalt through dacite suites of series B. However, this arc was farther east in Pliocene and Miocene times, and too distant from the Leg 124 sites. On the *Sulawesi Island*, subduction of the Indo-Australian Plate generated a large range of low-K to shoshonite suites since the early Miocene. Similar lavas constituted *the Sunda arc* since the Eocene to Holocene. This arc is a possible source for the oldest ash deposits cored at Leg 124.

In addition, calc-alkaline volcanic activities occurred along continental strips that separate marginal basins (Rangin, Silver, von Breymann et al., 1990). *The Palawan and the Cagayan Ridges* were the loci of a medium-K andesite volca-

nism related to subductions of the South China Sea passive margin, during the early to middle Miocene (Kudrass et al., 1990). *The Sulu Ridge* was active in the middle Miocene with subduction of the proto-South China Sea (Holloway, 1982), and since the Pliocene with subduction of the Sulu Sea. Lavas belong to series B: high-Al and medium-K andesite suites. At the nearby *North Sulawesi arc*, new subduction of the Celebes Sea since the late Miocene produced high-Al basalt suite (series B).

To sum up, the various arcs may be petrologically different in some parts (for example, shoshonitic feature of the Negros and central Mindanao volcanoes), but similar magmatic products occur in many distinct areas. There is little information concerning the magmatic evolution of these arcs through time and space (Bellon and Rangin, this volume). Different lava suites may be present at any time in the numerous and successive nearby volcanic arcs. The identity of the sources is inferred from stratigraphic correlations with known durations of volcanism on the arcs. Thus the Leg 124 record allows precise chronology of the explosive pulses in relation with the main volcano-tectonic events (Pubellier et al., this volume).

Considering the Leg 124 ash compositions, their stratigraphic ages, and the relative arc locations, possible sources are given in Table 6. Sites 767 and 770 may have been supplied by the Sunda, oldest Sulawesi, and Mindanao volcanoes in the Oligocene to early and middle Miocene (acidic volcaniclastites), and by the north Sulawesi, Sangihe, Mindanao, and Sulu volcanoes since the late Miocene (series A and B, basic to acidic tephra). Sites 768 and 769 were obviously supplied by the Cagayan Ridge at the early middle Miocene (hyaloclastite and pyroclastite flows) and by the west Philippine volcanoes, especially by the Negros volcanoes (series C), and the Sulu Archipelago since the mid-Pleistocene.

The Leg 124 Volcanic Record

Volcanic ash from the Celebes and Sulu Sea Basins provide a good record of the explosive activity of the neighboring arcs since the late Oligocene in the Celebes area and since the early Miocene in the Sulu area. This record is discussed in Pubellier et al., this volume. Chemical and petrological investigations are used to characterize volcanic pulses (Table 6). Notably, successive input of mafic to evolved magmatic products indicate three magmatic sequences: (1) in the early Pliocene, (2) in the late Pliocene to early Pleistocene, and (3) in the middle to late Pleistocene.

This new information provides additional data for palinspastic reconstructions of this western Pacific region (Rangin et al., 1990).

Late Oligocene-Early Miocene Time (Age Groups 10 and 9)

The Celebes Basin registered two pulses circa 32 and 25 Ma. Poorly characterized andesites and rhyolites may indicate activities of the Sunda arc and of the Sabah old Sulu arc.

Late Early and Middle Miocene Time (Age Groups 8 and 7)

Diluted volcaniclastic material in the Celebes Basin sediments indicates distant location of sources: Sulawesi to the south and Sulu to the north.

Sulu Sea andesitic through dacitic tuffs originated from the Cagayan volcanic chain circa 18–17 Ma. Hyaloclastites correspond to proximal flows whereas pyroclastites are attributed to more distal deposition of explosive tephra. This activity ended when the Cagayan and Palawan ridges collided with the Philippine Plate (Rangin, 1989; Rangin et al., 1990; Rangin and Pubellier, 1990). In the early late Miocene, circa 10 Ma, dacite to evolved rhyolite activity is registered in the Sulu Sea Basin.

Table 4. Chemical analyses and structural formulas of minerals.

	Table 4 - I - A														
	5	16	5'	8	11	24	22	24'	21	16'	13	25	27	16''	25'
SiO ₂	49.35	49.51	54.36	56.11	57.76	59.47	62.88	64.14	65.32	65.91	65.71	66.93	65.50	65.27	64.23
Al ₂ O ₃	30.27	28.88	27.23	26.38	25.05	23.71	22.39	20.29	19.75	19.06	18.20	17.72	17.18	16.85	16.94
Fe ₂ O ₃	0.59	0.95	0.73	0.68	0.57	0.87	0.66	0.12	0.23	0.26	0.53	0.19	0.36	0.07	0.00
CaO	16.45	14.69	12.05	10.89	8.34	7.66	4.71	3.03	2.54	2.56	0.83	0.33	0.13	0.00	0.00
Na ₂ O	1.85	3.16	4.36	5.16	5.89	6.72	8.04	9.96	10.36	7.24	6.21	6.31	3.27	1.09	0.27
K ₂ O	0.07	0.23	0.23	0.28	0.53	0.54	1.63	1.15	0.82	4.18	6.94	7.81	11.60	14.64	16.59
Total	98.58	97.42	98.96	99.50	98.14	98.97	100.31	98.69	99.02	99.21	98.42	99.29	98.04	97.92	98.03
Si	2.291	2.329	2.486	2.543	2.644	2.689	2.795	2.884	2.917	2.958	3.005	3.027	3.037	3.057	3.035
Al	1.656	1.601	1.468	1.409	1.351	1.264	1.173	1.075	1.040	1.008	0.981	0.945	0.939	0.930	0.944
Fe ³⁺	0.021	0.034	0.025	0.024	0.018	0.030	0.022	0.004	0.008	0.009	0.016	0.006	0.013	0.002	0.000
Ca	0.818	0.740	0.590	0.529	0.409	0.371	0.224	0.146	0.121	0.123	0.041	0.016	0.006	0.000	0.000
Na	0.167	0.288	0.387	0.454	0.523	0.589	0.693	0.868	0.897	0.630	0.551	0.553	0.294	0.099	0.025
K	0.004	0.014	0.013	0.016	0.031	0.031	0.093	0.066	0.047	0.240	0.406	0.452	0.688	0.877	1.002
An	82.74	71.03	59.62	52.97	42.48	37.43	22.21	13.51	11.41	12.40	4.08	1.56	0.66	0.00	0.00
Ab	16.84	27.65	39.03	45.4	54.30	59.42	68.62	80.37	84.20	63.45	55.23	54.20	29.75	10.15	2.40
Or	0.42	1.32	1.35	1.62	3.22	3.15	9.17	6.12	4.39	24.15	40.69	44.24	69.59	89.58	97.60
	Table 4 - I - B														
	32	34	47	37	32	44	40	51	29	42	47'	31			
SiO ₂	48.52	50.05	53.34	54.82	59.16	60.22	65.44	66.88	66.67	64.42	65.72	65.96			
Al ₂ O ₃	30.49	29.55	28.63	26.96	23.94	24.09	21.36	18.99	18.78	18.49	18.60	17.07			
Fe ₂ O ₃	0.74	1.19	0.88	0.17	0.52	0.72	0.18	0.23	0.12	0.53	0.00	0.10			
CaO	17.20	15.22	12.11	12.02	8.51	6.93	3.14	1.53	1.63	1.56	0.92	0.00			
Na ₂ O	1.45	2.85	4.30	5.47	6.75	7.12	9.11	10.70	7.86	3.81	3.56	2.39			
K ₂ O	0.01	0.15	0.09	0.11	0.17	0.71	1.52	0.10	4.10	9.18	9.41	13.44			
Total	98.41	99.01	99.35	99.55	99.05	99.79	100.75	98.43	99.16	97.99	98.21	98.96			
Si	2.262	2.316	2.432	2.496	2.673	2.695	2.873	2.979	2.984	2.974	3.008	3.049			
Al	1.675	1.612	1.538	1.447	1.275	1.271	1.105	0.997	0.991	1.007	1.003	0.930			
Fe ³⁺	0.029	0.046	0.030	0.006	0.020	0.024	0.006	0.008	0.005	0.020	0.000	0.004			
Ca	0.859	0.755	0.592	0.586	0.412	0.333	0.148	0.073	0.078	0.077	0.045	0.000			
Na	0.131	0.256	0.380	0.483	0.591	0.618	0.775	0.924	0.682	0.341	0.316	0.214			
K	0.000	0.009	0.005	0.006	0.010	0.040	0.085	0.006	0.234	0.541	0.551	0.793			
An	86.73	74.05	60.56	54.51	40.70	33.57	14.66	7.30	7.85	8.05	4.94	0.00			
Ab	13.23	25.09	38.91	44.89	58.35	62.35	76.89	92.12	68.59	35.56	34.66	21.26			
Or	0.40	0.86	0.53	0.60	0.95	4.08	8.45	0.58	23.56	56.39	60.40	78.74			
	Table 4 - I - C														
Sample	63	64	62	59	62'	67	62"	68							
SiO ₂	48.20	50.99	51.74	53.84	56.60	59.89	61.87	66.37							
Al ₂ O ₃	30.60	28.80	28.20	27.63	25.98	22.80	22.23	17.62							
Fe ₂ O ₃	0.94	0.91	0.98	0.98	0.52	0.38	0.35	0.38							
CaO	16.23	14.16	13.87	11.45	9.87	6.35	5.42	0.22							
Na ₂ O	1.81	3.11	3.52	4.85	5.80	7.54	7.80	4.34							
K ₂ O	0.06	0.11	0.27	0.43	0.31	0.91	1.28	10.34							
Total	97.84	98.08	98.58	99.18	99.08	97.87	98.95	99.27							
Si	2.258	2.371	2.395	2.461	2.569	2.730	2.785	3.026							
Al	1.689	1.578	1.539	1.488	1.390	1.225	1.179	0.947							
Fe ³⁺	0.037	0.035	0.038	0.038	0.020	0.015	0.013	0.015							
Ca	0.815	0.705	0.688	0.561	0.480	0.310	0.261	0.011							
Na	0.164	0.281	0.316	0.430	0.510	0.666	0.681	0.383							
K	0.004	0.067	0.016	0.025	0.018	0.053	0.074	0.601							
An	82.90	71.03	67.46	55.22	47.61	30.14	25.74	1.07							
Ab	16.71	28.29	30.96	42.31	50.60	64.74	67.02	38.53							
Or	0.39	0.67	1.58	2.47	1.79	5.12	7.24	60.41							
	Table 4 - II														
	5	6	8	11	13	13'	16	34	36						
SiO ₂	52.61	49.90	55.68	52.22	52.69	47.29	53.62	52.51	54.36						
Al ₂ O ₃	3.42	3.96	0.66	3.31	2.12	7.52	1.68	3.29	2.20						
Fe ₂ O ₃	0.00	1.13	0.00	0.74	0.88	4.01	0.00	0.28	0.00						
FeO	9.03	9.82	18.38	17.35	7.73	3.70	9.06	7.74	8.65						
MnO	0.24	0.19	1.04	0.69	0.51	0.08	0.56	0.24	0.26						
MgO	15.09	13.45	23.39	23.86	15.44	13.51	15.35	14.74	14.49						
CaO	19.83	19.07	1.34	1.51	20.59	21.99	19.93	21.20	20.69						
Na ₂ O	0.30	0.47	0.05	0.03	0.27	0.21	0.17	0.40	0.05						
TiO ₂	0.46	1.01	0.17	0.21	0.42	0.50	0.36	0.52	0.65						
Total	100.98	99.00	100.71	99.92	100.65	98.81	100.73	100.93	101.35						
Si	1.930	1.884	2.039	1.914	1.940	1.771	1.977	1.925	2.000						
Al IV	0.070	0.116	0.000	0.086	0.060	0.229	0.023	0.075	0.000						
Al VI	0.078	0.060	0.028	0.056	0.032	0.103	0.050	0.067	0.095						
Fe ³⁺	0.000	0.032	0.000	0.020	0.024	0.113	0.000	0.008	0.000						
Fe ²⁺	0.288	0.310	0.562	0.531	0.238	0.116	0.279	0.237	0.265						

Table 4 (continued).

Mn	0.007	0.006	0.032	0.021	0.016	0.002	0.017	0.007	0.008
Mg	0.825	0.757	1.277	1.303	0.847	0.754	0.844	0.805	0.795
Ca	0.779	0.771	0.052	0.059	0.812	0.882	0.787	0.833	0.815
Na	0.021	0.034	0.003	0.002	0.019	0.015	0.012	0.028	0.004
Ti	0.013	0.029	0.005	0.006	0.012	0.014	0.010	0.014	0.018
Wo	35.90	34.22	2.06	1.50	38.17	33.36	38.18	38.58	39.73
En	41.38	37.86	65.71	65.17	42.37	37.71	42.57	40.28	41.03
Fs	14.24	15.78	30.57	27.62	12.68	5.91	14.95	12.22	14.13
Jd	2.14	0.22	0.36	0.00	0.00	0.00	1.23	2.06	0.37
Ac	0.00	3.22	0.00	0.21	1.93	1.52	0.00	0.79	0.00
Ca-Tsch	5.07	5.83	0.80	3.09	3.19	10.30	2.06	4.64	2.88
Fa-Tsch	0.00	0.00	0.00	1.83	0.50	9.78	0.00	0.00	0.00
Ti-Tsch	1.27	2.87	0.48	0.58	1.16	1.41	1.01	1.43	1.86

Table 4 - II

	50	54	54'	62	62'	64	65	70	
SiO ₂	54.12	51.35	51.94	55.08	51.76	53.27	55.15	52.87	
Al ₂ O ₃	1.32	2.87	3.41	2.26	2.72	2.33	0.73	1.95	
Fe ₂ O ₃	0.10	1.00	1.84	0.00	1.89	0.00	0.00	0.00	
FeO	19.92	8.61	2.70	13.02	8.87	8.12	14.51	9.53	
MnO	0.97	0.28	0.18	0.68	0.57	0.50	0.66	0.28	
MgO	23.54	14.91	16.47	27.61	14.95	14.96	26.74	15.19	
CaO	1.44	19.60	22.89	0.64	19.28	19.86	1.06	20.67	
Na ₂ O	0.03	0.29	0.18	0.00	0.35	0.32	0.06	0.15	
TiO ₂	0.12	0.56	0.31	0.40	0.57	0.33	0.14	0.14	
Total	101.57	99.47	99.92	99.89	100.97	99.69	99.05	100.78	
Si	1.968	1.918	1.899	1.974	1.911	1.979	2.007	1.948	
Al IV	0.032	0.082	0.101	0.026	0.089	0.021	0.000	0.062	
Al VI	0.025	0.044	0.045	0.069	0.030	0.081	0.031	0.022	
Fe ³⁺	0.003	0.028	0.050	0.000	0.053	0.000	0.000	0.000	
Fe ²⁺	0.605	0.268	0.082	0.389	0.274	0.252	0.441	0.293	
Mn	0.030	0.009	0.006	0.021	0.018	0.016	0.020	0.009	
Mg	1.276	0.830	0.898	1.485	0.823	0.829	1.451	0.834	
Ca	0.056	0.784	0.897	0.025	0.762	0.790	0.041	0.816	
Na	0.002	0.021	0.013	0.000	0.025	0.023	0.004	0.011	
Ti	0.003	0.016	0.008	0.011	0.016	0.009	0.004	0.004	
Wo	1.37	35.86	39.94	1.10	34.48	38.07	1.41	38.74	
En	63.81	41.50	44.80	75.49	41.15	42.02	73.45	41.50	
Fs	31.74	13.86	4.39	20.84	14.57	13.57	23.25	15.02	
Jd	0.00	0.00	0.00	0.00	0.00	2.34	0.43	1.07	
Ac	0.21	2.10	1.27	0.00	2.51	0.00	0.00	0.00	
Ca-Tsch	2.46	4.39	4.22	2.68	2.96	3.07	0.98	3.29	
Fa-Tsch	0.08	0.71	4.52	0.00	2.76	0.00	0.00	0.00	
Ti-Tsch	0.33	1.57	0.85	1.10	1.58	0.93	0.39	0.39	

Table 4 - III

	1	3	8	13	14	19	33	37	
SiO ₂	46.58	54.37	47.71	44.27	44.14	45.01	49.41	43.11	
Al ₂ O ₃	8.82	6.09	7.79	10.94	12.41	10.02	7.01	13.47	
Fe ₂ O ₃	8.64	6.40	3.84	5.63	7.04	5.65	7.01	5.14	
FeO	4.31	4.16	8.30	7.34	4.67	9.19	6.75	3.88	
MnO	0.33	0.37	0.38	0.29	0.25	0.59	0.38	0.24	
MgO	14.50	15.79	14.44	13.70	14.85	12.44	14.92	15.58	
CaO	10.62	9.67	10.99	11.53	11.65	10.84	10.96	12.07	
Na ₂ O	1.66	1.10	2.06	2.18	2.36	2.04	1.79	2.51	
K ₂ O	0.29	0.27	0.37	0.53	0.54	0.82	0.38	0.45	
TiO ₂	1.38	0.59	2.12	1.20	1.47	2.18	1.24	1.30	
Total	97.13	98.81	97.99	97.61	99.39	98.78	99.85	97.75	
Si	6.727	7.509	6.880	6.459	6.276	6.543	6.975	6.193	
Al	1.501	0.991	1.324	1.881	2.080	1.717	1.166	2.281	
Fe ³⁺	0.939	0.665	0.417	0.619	0.753	0.618	0.745	0.555	
Fe ²⁺	0.521	0.481	1.000	0.896	0.556	1.117	0.797	0.466	
Mn	0.040	0.043	0.046	0.036	0.030	0.073	0.045	0.029	
Mg	3.121	3.250	3.103	2.979	3.147	2.695	3.139	3.335	
Ca	1.643	1.431	1.698	1.802	1.775	1.688	1.658	1.858	
Na	0.465	0.295	0.576	0.617	0.651	0.575	0.490	0.699	
K	0.054	0.048	0.068	0.099	0.098	0.152	0.069	0.083	
Ti	0.150	0.061	0.230	0.132	0.157	0.238	0.132	0.140	
Mg/Mg + Fe ²⁺	84.76	86.12	74.78	76.18	84.31	69.37	78.84	87.08	

Table 4 - III

	41	45	48	48'	64	68	70	
SiO ₂	47.90	48.82	48.35	45.35	43.98	49.77	50.37	
Al ₂ O ₃	8.33	7.76	7.45	10.83	10.35	6.59	5.59	
Fe ₂ O ₃	14.25	10.57	10.36	8.42	6.17	8.59	9.99	

Table 4 (continued).

FeO	0.01	2.43	3.42	2.12	12.52	6.42	2.80
MnO	0.37	0.33	0.27	0.21	0.63	0.16	0.35
MgO	14.85	15.53	15.26	15.86	10.25	14.14	16.40
CaO	9.36	10.42	10.57	10.90	11.30	10.42	10.78
Na ₂ O	1.49	1.47	1.54	2.24	1.48	1.40	1.23
K ₂ O	0.15	0.25	0.14	0.36	1.37	0.09	0.10
TiO ₂	1.03	0.97	1.54	1.59	1.05	1.22	1.14
Total	97.74	98.55	98.90	97.87	98.48	98.80	98.75
Si	6.793	6.890	6.838	6.462	6.505	7.071	7.086
Al	1.392	1.291	1.242	1.819	1.804	1.104	0.927
Fe ³⁺	1.520	1.123	1.102	0.903	0.686	0.918	1.057
Fe ²⁺	0.001	0.287	0.405	0.252	1.549	0.763	0.329
Mn	0.044	0.039	0.032	0.025	0.079	0.019	0.042
Mg	3.139	3.267	3.216	3.368	2.259	2.994	3.438
Ca	1.422	1.576	1.602	1.664	1.791	1.568	1.625
Na	0.410	0.402	0.422	0.619	0.424	0.386	0.335
K	0.027	0.045	0.025	0.067	0.259	0.016	0.018
Ti	0.110	0.103	0.164	0.170	0.117	0.130	0.121
Mg/Mg + Fe ²⁺	98.57	90.92	88.04	92.39	58.12	79.28	90.25

Table 4 - IV

	8	25	25'	28	33	36	40	40'	43	50	62	68
SiO ₂	0.58	0.45	0.26	0.85	0.52	1.10	0.74	0.84	0.00	0.00	2.93	1.08
Al ₂ O ₃	1.48	2.02	0.68	2.06	2.00	3.32	2.05	0.71	0.28	0.18	4.76	2.32
Fe ₂ O ₃	48.39	48.05	47.62	36.61	56.80	49.80	57.58	47.64	21.36	10.94	48.80	50.78
FeO	38.39	35.58	23.54	40.78	33.18	33.71	32.94	22.68	29.61	38.99	31.88	35.50
MnO	0.55	0.94	0.41	0.85	0.61	0.59	0.37	0.42	1.12	0.89	0.30	0.63
MgO	0.49	2.03	0.36	2.68	1.65	2.34	1.33	0.66	3.92	1.56	4.05	1.74
CaO	0.06	0.00	0.00	0.06	0.13	0.17	0.03	0.00	0.00	0.00	0.21	0.11
TiO ₂	9.46	9.52	26.81	15.85	5.44	7.64	4.64	26.46	41.74	47.32	7.84	8.21
Total	99.40	98.59	99.67	99.74	100.33	98.67	99.68	99.41	98.03	99.88	100.77	100.37
Si	0.175	0.135	0.013	0.249	0.154	0.326	0.221	0.043	0.000	0.000	0.820	0.318
Al	0.527	0.715	0.041	0.710	0.700	1.158	0.123	0.043	0.017	0.011	1.570	0.804
Fe ³⁺	10.994	10.854	1.848	8.059	12.696	11.090	12.964	1.841	0.811	0.413	10.279	11.233
Fe ²⁺	9.693	8.932	1.015	9.977	8.242	8.343	8.242	0.974	1.249	1.637	7.462	8.727
Mn	0.141	0.239	0.018	0.211	0.153	0.148	0.094	0.018	0.048	0.038	0.071	0.157
Mg	0.221	0.908	0.027	1.168	0.730	1.032	0.593	0.051	0.295	0.117	1.689	0.762
Ca	0.019	0.000	0.000	0.019	0.041	0.054	0.010	0.000	0.000	0.000	0.063	0.035
Ti	2.148	2.149	1.040	3.487	1.215	1.700	1.044	1.022	1.583	1.786	1.650	1.815

Table 4 - V

	17	31	37
SiO ₂	37.89	39.11	39.09
Al ₂ O ₃	13.07	12.23	13.15
FeO	17.50	15.56	12.20
MnO	0.26	0.28	0.04
MgO	13.79	14.75	16.87
CaO	0.00	0.00	0.30
Na ₂ O	0.31	0.44	0.84
K ₂ O	8.90	9.27	7.60
TiO ₂	3.91	3.37	3.21
H ₂ O	3.71	3.37	4.02
Total	99.34	99.00	97.31
Si	5.703	5.873	5.825
Al	2.319	2.165	2.309
Fe ²⁺	2.203	1.954	1.521
Mn	0.033	0.036	0.005
Mg	3.093	3.301	3.747
Ca	0.000	0.000	0.048
Na	0.090	0.128	0.241
K	1.713	1.780	1.444
Ti	0.443	0.381	0.360
H ₂ O	2.000	2.000	2.000
Mg/Mg + Fe ²⁺	58.04	62.39	71.05
+ Mn			

5

SiO ₂	39.92
FeO	18.73
MnO	0.13
MgO	41.06
CaO	0.15
TiO ₂	0.00
Total	99.99

Table 4 (continued).

Si	1.017
Fe ²⁺	0.399
Mn	0.003
Mg	1.559
Ca	0.004
Ti	0.000
Mg/Mg + Fe ²⁺ + Mn	79.50
	9
SiO ₂	37.65
Al ₂ O ₃	22.89
Fe ₂ O ₃	12.67
MnO	0.27
MgO	0.12
CaO	22.66
Na ₂ O	0.00
K ₂ O	0.00
TiO ₂	0.18
Total	96.44
Si	2.914
Al	2.088
Fe ³⁺	0.738
Mn	0.018
Mg	0.014
Ca	1.879
Na	0.000
K	0.000
Ti	0.010

Sample numbers are from Table 1. I—feldspars (A, Sites 767, 770; B, Site 768; C, Site 769; in the An-decreasing order). II, pyroxenes. III, amphiboles. IV, magnetites and ilmenites. V, biotites, olivine and epidote.

At that time the Philippine arc (carried by the Philippine Plate) collided with the Eurasian margin.

Late Miocene and Early Pliocene Time (Age Groups 6 and 5)

In the late Miocene, renewal of volcanic activity is indicated at the two basins since 8–7.5 Ma. Magmatic compositions are poorly defined. A better record is registered at all the sites in the early Pliocene (magmatic sequence I, Table 6). This is in agreement with the new tectonic setting that followed the major compression event in the late late Miocene: left-lateral movement of the Philippine fault, reversal of subduction orientation beneath Sulu Archipelago, subduction of the Philippine Sea, and beginning closure of the Molucca Sea (Divis, 1980; Cardwell and Isacks, 1981; Mukasa et al., 1987; Rangin, Silver, von Breymann, et al., 1990). Celebes Sea ash layers give evidence of newly born volcanoes of the Sangihe immature arc (type A fractionation trend). Sulu Sea sites denote activity of the new Sulu-Zamboanga arc and of the Negros volcanoes.

Late Pliocene-Middle Pleistocene Time (Age Groups 4 and 3)

The apparent absence of volcanic ash between 3.5–2.5 Ma may be explained, partly, by dissolution of vitric glasses (Desprairies et al., this volume), or by the period of absence of activity between the Sangihe subduction and the Cotobato trench in Mindanao (Pubellier et al., in press). We may assume that tectonic constraints are limited to strike-slip movements in the central Philippines. However, a new volcano-tectonic pulse occurred at 2.5 Ma (magmatic sequence II, Table 6). In the Celebes Sea Basin, from late Pliocene to mid-Pleistocene time, the two magmatic compositions of ashes denote an activity of the Sangihe arc or the North Sulawesi arc and a contribution from the Mindanao and the Sulu volcanoes. In the Sulu Sea Basin, ash beds registered

moderate activity from the Sulu-Zamboanga arc and from the Negros volcanoes.

Middle Pleistocene-Holocene Time (Age Groups 2 and 1)

The last important magmatic phase occurred in the late Pleistocene (sequence III, Table 6), with renewal of all the present south Philippine arcs: Cotobato and Sulu (Sites 767 and 770), and Sulu and Negros (Sites 768 and 769). This phase is still continuing, to a lesser extent, giving mafic products from nearby volcanic chains and episodic acidic explosive tephra dispersed in sea basins.

CONCLUSION

The volcaniclastic material recovered during Leg 124 in the Celebes and Sulu Sea Basins gives a good record of the nearby volcanic arc activities since the Oligocene. The material originated from Vulcanian to Plinian explosive eruptions and was deposited as fallout ash layers in the sedimentary pile of the two basins and as pyroclastite flows in Miocene strata of the Sulu Basin.

Mineralogical and geochemical studies of 70 samples lead us to distinguish three magmatic series: (1) low-alumina and medium-K andesitic series, (2) high-alumina and medium-K basalt series, and (3) high-alumina and high-K andesitic to shoshonitic series. Some volcanic suites occurred at various places and times in the numerous surrounding volcanic arcs and ridges.

In a first step, the identity of the sources is inferred from stratigraphic correlations with known durations of volcanism on the arcs. Thus the Leg 124 record allows a precise chronology of the volcanic pulses. In a second step, interesting information is deducted from the volcanological and petrological investigations. The Sulu Sea hyaloclastite and pyroclastite tuffs originated

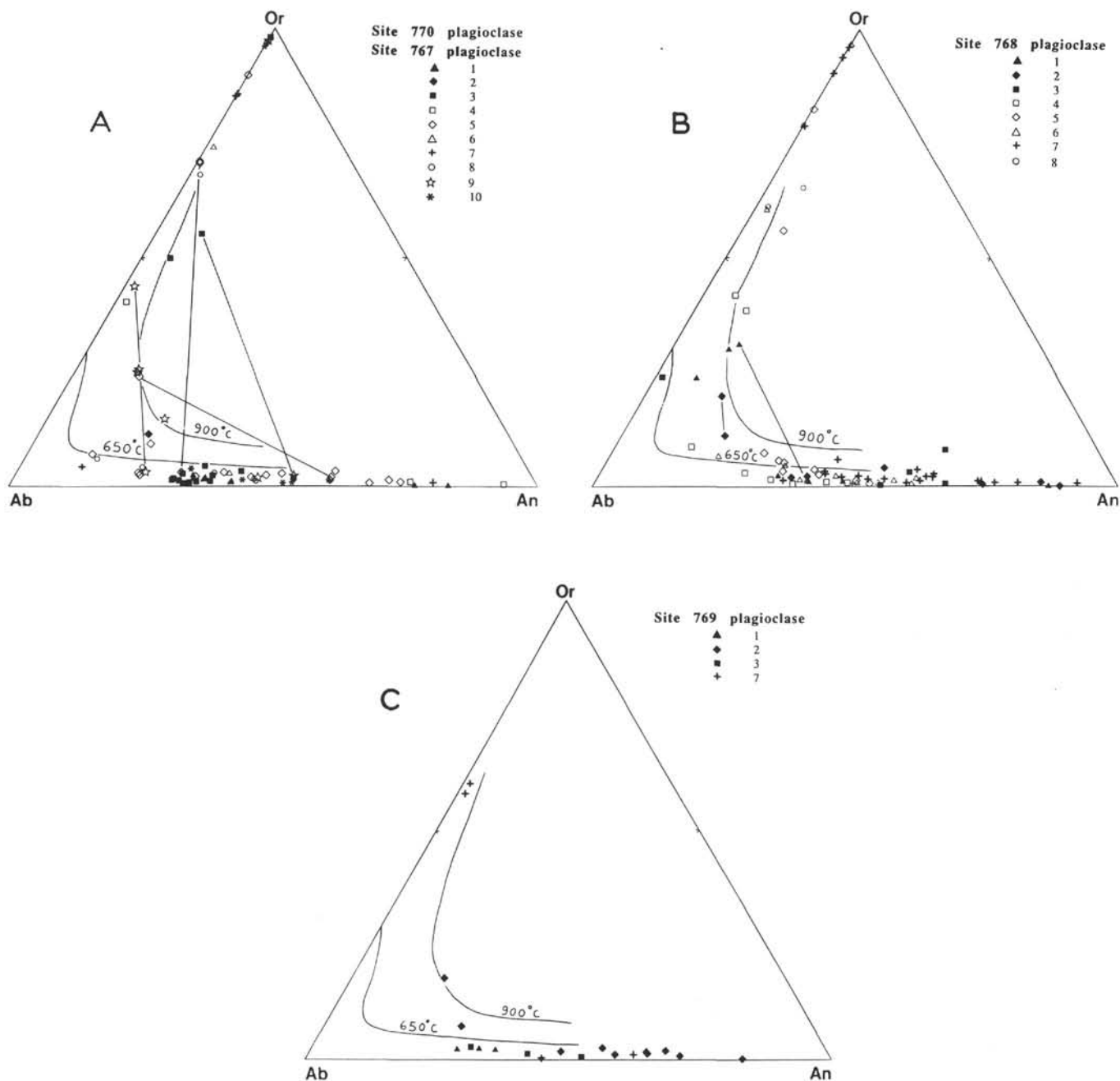


Figure 5. An-Ab-Or diagram of the feldspars. A. Sites 767, 770. B. Site 768. C. Site 769. 1 to 10, symbols for the age groups. Tie-lines join coexisting feldspars. Limits of feldspar solid solutions at $P\ H_2O = 1$ kbar for 900°C and 650°C according to Seck (1971).

from the Cagayan volcanic chain in the early middle Miocene. After that, the Cagayan ridge activity stopped. Low-alumina hornblende-andesite lava suites are recorded when a new arc becomes active (Sangihe-north-Sulawesi). A more complex magmatic activity (three sequences) is distinguished in the Pliocene-Pleistocene. This may correspond to successive stages in the new tectonic setting that followed the major compression event in the late late Miocene.

ACKNOWLEDGMENT

We greatly appreciate conspicuous and highly pertinent suggestions and questions from the two reviewers, James Natland and Richard Fisher, and from Claude Rangin. We

thank Michel Tallet for his skillful participation in the microprobe analyses. This research was supported by a CNRS grant (ODP-France).

REFERENCES

- Andersen, D. J., and Lindsley, D. H., 1988. Internally consistent solution models for Fe-Mg-Mn-Ti oxides: Fe-Ti oxides. *Am. Mineral.*, 73:714-726.
- Barth, T.F.W., 1962. Feldspar solid solutions. *Chem. Erde*, 22:31.
- Cardwell, R. K., and Isacks, B. L., 1981. A review of the configuration of the Eastern Indonesian and Philippine islands. In *The Geology and Tectonics of Eastern Indonesia*. Geol. Res. Develop. Centre, Spec. Publ., 2:31-72.

- Divis, A. F., 1980. The petrology and tectonics of recent volcanism in the Central Philippine islands. In Hayes, D. E. (Ed.), *The Tectonic and Geologic Evolution of Southeast Asian Seas and Islands*. Am. Geophys. Union., Geophys. Monogr., 27:127-144.
- Fisher, R. V., 1961. Proposed classification of volcaniclastic sediments and rocks. *Geol. Soc. Am. Bull.*, 72:1409-1414.
- Fisher, R. V., 1966. Rocks composed of volcanic fragments and their classification. *Earth-Sci. Rev.*, 1:287-298.
- Fisher, R. V., and Schmincke, H.-U., 1984. *Pyroclastic Rocks*: New York (Springer-Verlag).
- Hall, R., Audley-Charles, M. G., Banner, F. T., Hidayat, S., and Tobing, S. L., 1988. Late Paleogene-Ouaternary geology of Halmahera, Eastern Indonesia: initiation of a volcanic island arc. *J. Geol. Soc. London*, 145:577-590.
- Hammarstrom, J. M., and Zen, E.-A., 1986. Aluminium in hornblende: an empirical igneous geobarometer. *Am. Mineral.*, 71:1297-1313.
- Hollister, L. S., Grimssom, G. C., Peters, E. K., Stowell, H. H., and Sisson, V. B., 1987. Confirmation of the empirical correlation of Al in hornblende with pressure of solidification of calc-alkaline plutons. *Am. Mineral.*, 72:231-239.
- Holloway, N. H., 1982. The stratigraphy and tectonic relationship of Reed Bank, North Palawan, and Mindoro to the Asian Mainland and its significance in the evolution of the South China Sea. *AAPG Bull.*, 66:1357-1383.
- Huang, T. C., 1980. A volcanic sedimentation model: implication of processes and responses of deep-sea ashes. *Mar. Geol.*, 38:103-122.
- Jezeck, P. A., Whitford, D. J., and Gill, J. B., 1981. Geochemistry of recent lavas from the Sangihe-Sulawesi arc, Indonesia. In *The Geology and Tectonics of Eastern Indonesia*. Geol. Res. Dev. Cent. Spec. Publ., 2:383-389.
- Kudo, A. M., and Weill, D. F., 1970. An igneous plagioclase thermometer. *Contrib. Mineral. Petrol.*, 25:52-65.
- Kudrass, H. R., Müller, P., Kreuzer, H., and Weiss, W., 1990. Volcanic rocks and tertiary carbonates dredged from the Cagayan Ridge and the Southwest Sulu Sea, Philippines. In Rangin, C., Silver, E. A., von Breymann, M. T., et al., *Proc. ODP, Init. Repts.*, 124: College Station, TX (Ocean Drilling Program), 93-100.
- Mathez, E. A., 1973. Refinement of the Kudo-Weill plagioclase thermometer and its application to basaltic rocks. *Contrib. Mineral. Petrol.*, 41:61-72.
- Morris, J. D., Jezeck, P. A., Hart, S. R., and Gill, J. B., 1983. The Halmahera island arc, Molucca Sea collision zone, Indonesia: a geochemical survey. In Hayes, D. E. (Ed.), *The Tectonic and Geologic Evolution of Southeast Asian Seas and Islands* (Pt. 2). Am. Geophys. Union., Geophys. Monogr., 27:373-387.
- Mukasa, S. B., McCabe, R., and Gill, J. B., 1987. Pb-isotopic compositions of volcanic rocks in the West and East Philippine island arcs: presence of the Dupal isotopic anomaly. *Earth Planet. Sci. Lett.*, 84:153-164.
- Pouclet, A., Cadet, J.-P., Fujioka, K., and Bourgois, J., 1985. Ash layers from Deep Sea Drilling Project Leg 84: Middle America Trench transect. In von Huene, R., Aubouin, J., et al., *Init. Repts. DSDP*, 84: Washington (U.S. Govt. Printing Office), 609-618.
- Pouclet, A., Cambray, H., Cadet, J.-P., Bourgois, J., and De Wever, P., 1990. Volcanic ash from Leg 112 off Peru. In Suess, E., von Huene, R., et al., *Proc. ODP, Sci. Results*, 112: College Station, TX (Ocean Drilling Program), 465-480.
- Pubellier, M., Quebral, R., Rangin, C., Deffontaines, B., Muller, C., Butterlin, J., and Manzano, J., in press. The Mindanao collision zone: a soft collision event within a continuous Neogene strike slip setting. *Spec. Iss. J. South East Asian Earth Sci.*
- Rangin, C., 1989. The Sulu Sea, a back-arc basin setting within a Neogene collision zone. *Tectonophysics*, 161:119-141.
- Rangin, C., Jolivet, L., Pubellier, M., and Tethys Pacific Working Group, 1990. A simple model for the tectonic evolution of Southeast Asia and Indonesia regions for the past 43 Ma. *Bull. Soc. Geol. Fr.*, 6:887-905.
- Rangin, C., Pubellier, M., 1990. Subduction and accretion of oceanic fragments along the Eurasian margin: southern Japan-Philippine region. Some constraints for continental growth. In Aubouin, J., and Bourgois, J. (Eds.), *Tectonics of Circum Pacific Continental Margins*, (V.S.P International Publ.), 139-144.
- Rangin, C., Silver, E., von Breymann, M. T., et al., 1990. *Proc. ODP, Init. Repts.*, 124: College Station, TX (Ocean Drilling Program).
- Rangin, C., Stephan, J.-F., Butterlin, J., Bellon, H., Müller, C., and Chorowicz, J., in press. Collision néogène d'arcs volcaniques dans le centre des Philippines. Stratigraphie et structure de la chaîne d'Antique, île de Panay. *Bull. Soc. Geol. Fr.*
- Seck, H. A., 1971. Koexistierende alkali-feldspate und plagioklase im System NaAlSi₃O₈-KAlSi₃O₈-CaAl₂Si₂O₈-H₂O bei Temperaturen von 650°C bis 900°C. *Neues Jahrb. Mineral. Abh.*, 115:315-395.
- Stormer, J. C., Jr., 1983. The effects of recalculation on estimates of temperature and oxygen fugacity from analyses of multicomponent iron-titanium oxides. *Am. Mineral.*, 68:586-594.
- Wells, P.R.A., 1977. Pyroxene thermometry in simple and complex systems. *Contrib. Mineral. Petrol.*, 62:129-139.
- Wolfe, J. A., 1981. Philippine geochronology. *J. Soc. Geol. Phil.*, 35:1-30.
- Wones, D. R., and Eugster, H. P., 1965. Stability of biotite: experiment, theory and application. *Am. Mineral.*, 50:1228-1272.
- Wright, T. L., and Doherty, P. C., 1970. A linear programming and least squares computer method for solving petrologic mixing problems. *Geol. Soc. Am. Bull.*, 81:1995-2008.
- Yuwono, Y. S., 1987. Contribution à l'étude du volcanisme potassique de l'Indonésie. Exemples du sud-ouest de Sulawesi et du volcan Muria (Java) [Ph.D. dissertation]. Univ. Brest, France.

Date of initial receipt: 19 June 1990

Date of acceptance: 18 February 1991

Ms 124B-144

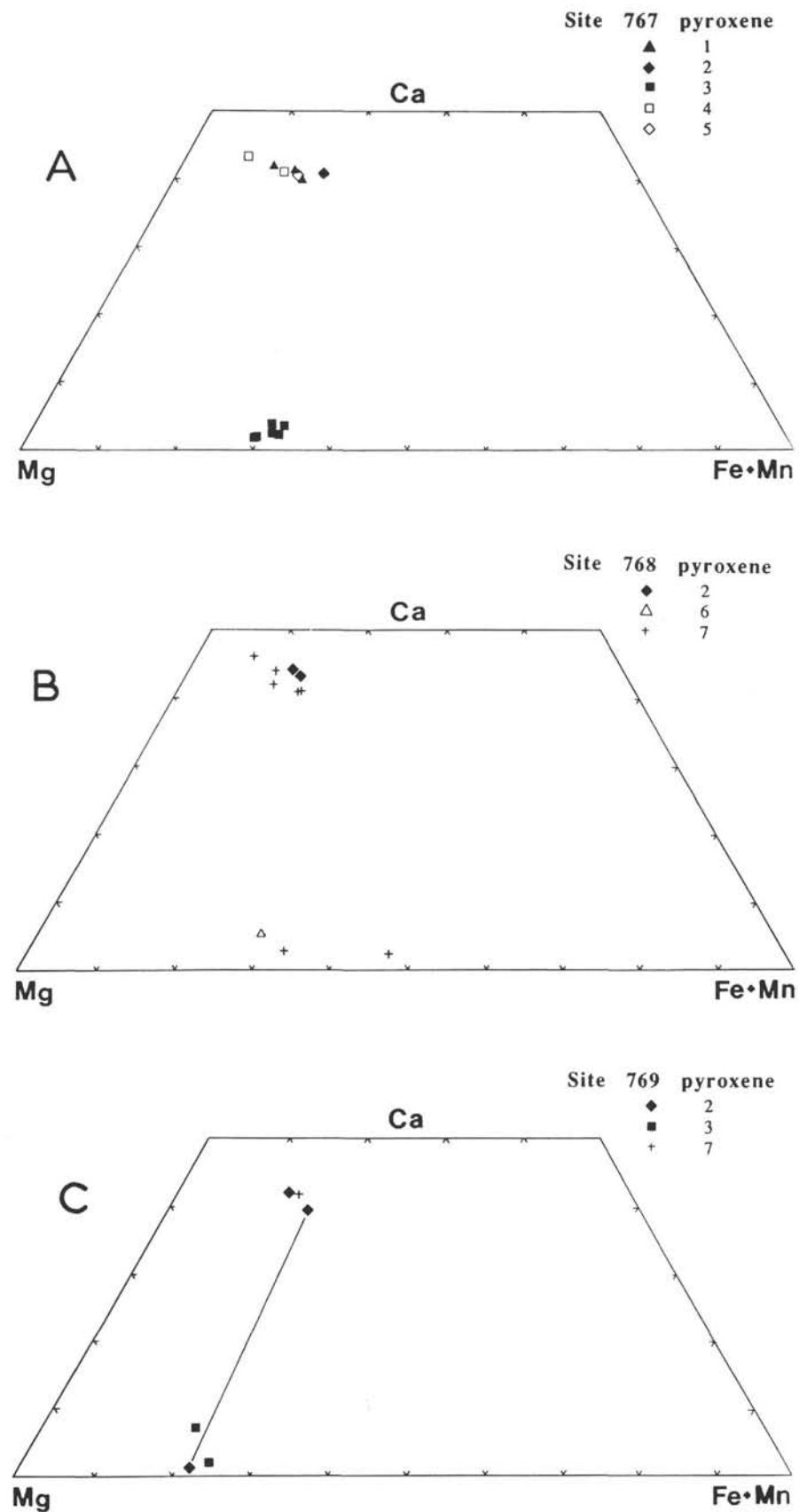


Figure 6. Mg-Ca-Fe + Mn diagram of the pyroxenes. A. Site 767. B. Site 768. C. Site 769. Numbers 1 to 10 show age groups. Tie-lines join coexisting pyroxenes.

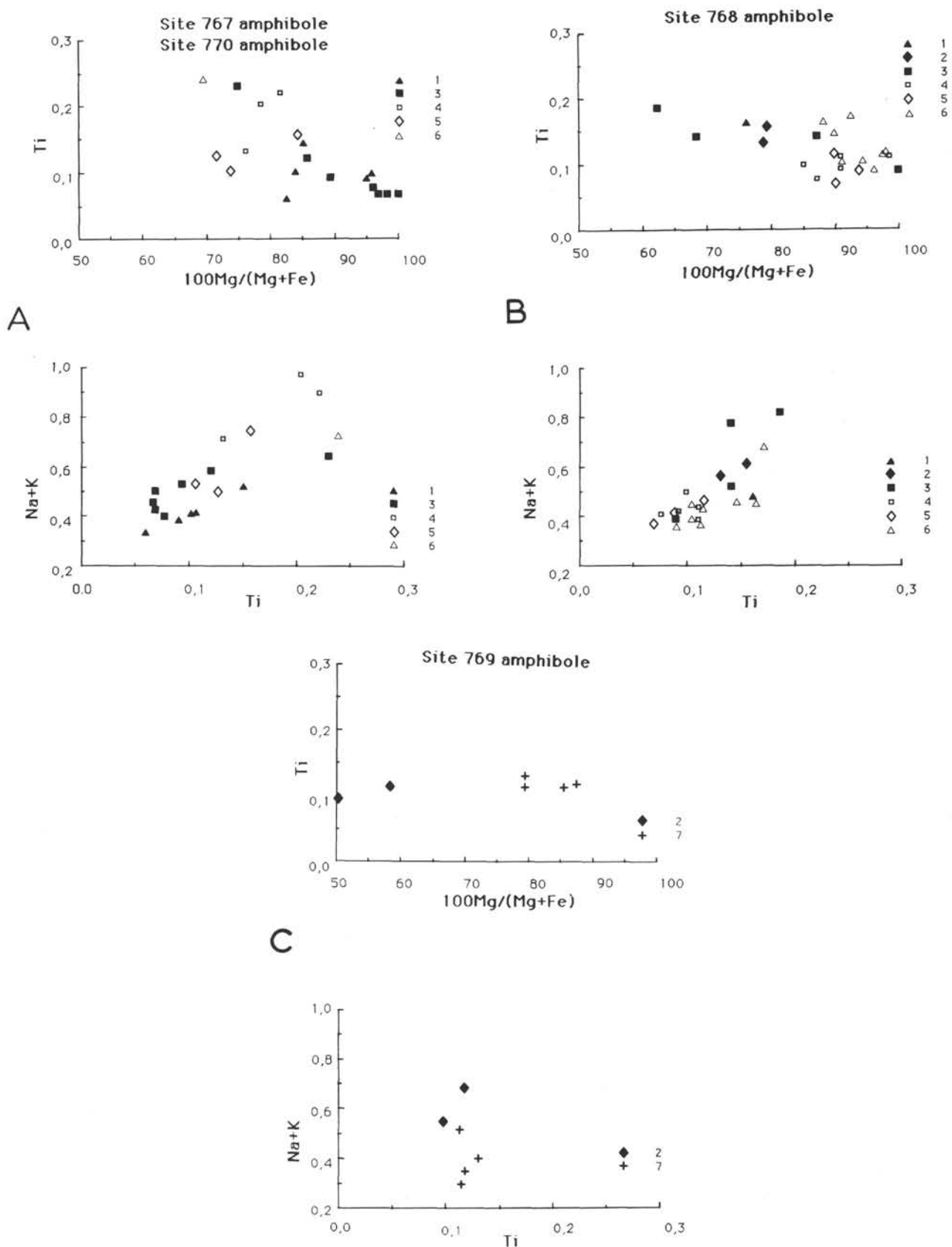


Figure 7. $100 \text{ Mg}/(\text{Mg} + \text{Fe})$ vs. Ti and Ti vs. $\text{Na} + \text{K}$ diagrams for amphibole determination. A. Sites 767, 770. B. Site 768. C. Site 769. Numbers 1 to 10 show age groups.

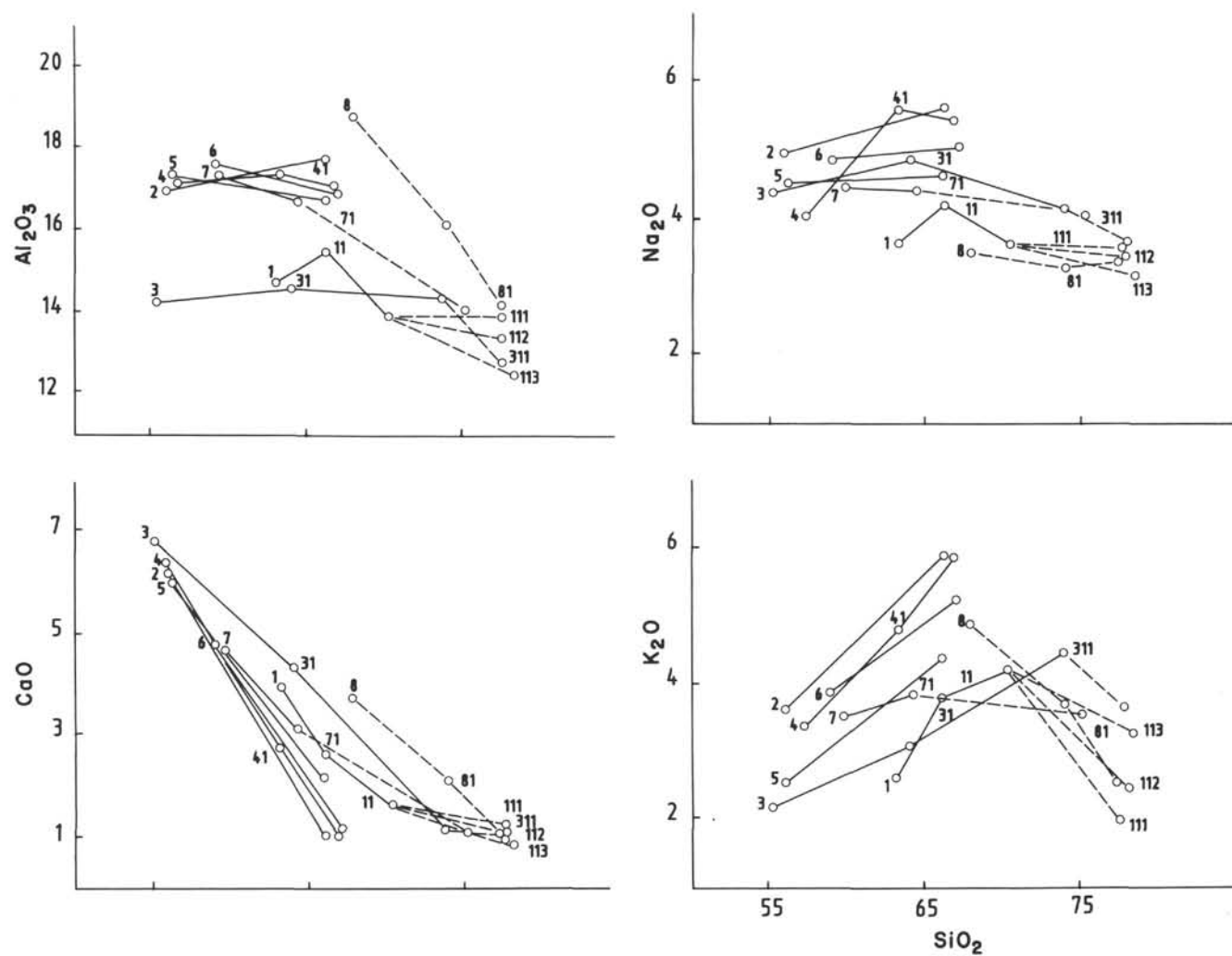


Figure 8. SiO_2 vs. Al_2O_3 , CaO , Na_2O , and K_2O crystallization trends (see text).

Table 5. Selected least-square mass balance calculations.

Site	Trend	Sample no. parent-daug.	Age group	% Fractionated minerals					Residual squared	% daughter
				CPX	Mt	Am	Bi	Pl		
767	1	14.1-14.2	5	6.4	4.0	—	5.4 (4)	—	0.871	84.2
	11	14.2-14.3	5	—	2.0	4.8(H)	—	10.5 (4)	18.5 (6)	0.652
	111	14.3-9	5-3	—	4.5	—	0.5	—	28.9 (9)	0.556
	112	14.3-10	5-3	—	4.4	—	0.7	—	27.3 (9)	0.829
	113	14.3-3	5.1	—	4.3	—	1.2	10.5 (4)	20.0 (9)	0.418
769	2	62.1-62.2	2	11.3	5.2	9.0(P)	—	22.5 (2)	—	1.800
769	3	64.1-64.2	2	1.0	4.5	24.2(P)	—	7.8 (1)	—	0.588
	31	64.2-64.3	2	12.4	4.6	—	—	27.9 (5)	—	1.166
	311	64.3-61	2-1	—	—	—	2.5	—	25.2 (8)	0.530
768	4	35.1-35.2	2	8.0	5.1	3.7(P)	—	16.1 (1)	—	0.878
	41	35.2-35.3	2	—	1.4	6.3(P)	—	16.3 (4)	—	0.174
769	5	67.1-67.2	3	—	4.6	19.9(P)	—	22.6 (2)	—	1.261
767	6	6.1-6.2	2	0.7	3.1	11.6(P)	—	19.8 (1)	—	0.873
769	7	66.1-66.2	3	3.2	2.5	—	5.8	25.0 (4)	—	0.547
	71	66.2-65	3	2.5	2.8	—	7.8	27.7 (4)	18.9 (7)	0.548
	71'	66.2-65	3	—	2.6	—	9.7	33.7 (4)	8.1 (10)	0.617
768	8	52-53	7	—	—	—	1.3	20.1 (1)	21.1 (10)	0.124
	81	53-51	7	—	—	—	—	11.5 (3)	14.1 (10)	0.440

Trend and age, see text. Sample no. from Table 2. Mineral analyses from Table 4: H, hornblende; P, pargasite. (1) to (10), feldspar compositions: 1, An60-Or1.4; 2, An50-Or5; 3, An45-Or5; 4, An35-Or4.3; 5, An20-Or10; 6, Or24-An12; 7, Or41-An5.7; 8, Or45-An5; 9, Or55-An11; 10, Or71-An0.4.

Abbreviations: daug, daughter; CPX, clinopyroxene; Mt, magnetite; Am, amphibole; Bi, biotite; Pl, plagioclase; F, alkaline feldspar.

Table 6. Petrochemical features of the successive volcanic activities according to the recorded tephra, and their possible location.

	Age groups and range (Ma)	Magmatic sequences	V	MS	Sites 767,770 Celebes	V	MS	Site 768 Sulu	Site 769 Cagayan
QUATERNARY	1 2 3 4 5 (3.5-5) 6 (5-8) 7 (9.5-12) 8 (17-18) 9 (~25) 10 (~32)	III II I	B A-B B A	(AND)-RH high-Al,-K AND-RH (Sangihe, Mindanao) high & low-Al,-K AND-RH rare high-Al,-K AND (Mindanao, Sulu) low-Al,-K AND-RH (Sangihe, N-Sulawesi) (DC) (RH) distant arcs location or dilution of ashes (DC-RH) AND-RH (Sabah-Zamboanga) RH (Sunda) mid-Eocene basement	B-C B B-C B-C B-C B-C B-C B-C B-C B-C	(DC)-RH high-Al,-K AND-RH (Negros, Sulu) (AND-DC)-RH (DC)-RH AND-RH (Sulu, Zamboanga) (AND)-DC-RH (Sulu, Zamboanga) pyroclastites tuffs (AND)-DC-RH early Miocene basement	(RH-DC) high-Al, -K AND-RH (Negros, Sulu) high-Al, medium-K AND-RH high-Al, medium-K AND-RH AND-RH (Sulu, Zamboanga, Negros) (AND)-RH (Sulu) (AND)-DC-RH (Sulu, Zamboanga) hyaloclastites tuffs AND-DC (Cagayan)		
late									
PLIOCENE									
early									
late									
MIOCENE									
middle									
early									
late									
OLIGOCENE									
early									